Axon guidance in the development of mammalian retinofugal pathways.

Kong Fung WONG

New Asia College

Thesis submitted for the degree of Master of Philosophy

Basic Medical Sciences

Department of Anatomy

The Chinese University of Hong Kong

June, 1997

Abstract :

Axon guidance in the development of mammalian retinofugal pathways.

Kong Fung WONG, New Asia College

Thesis submitted for the degree of Master of Philosophy
at Chinese University of Hong Kong

(June, 1997)

The primary goal of this thesis is to understand the guidance cues involved in the development of the retinofugal pathway. Three appraoches were used in order to understand the development of the retinofugal pathway and also the cues involved in the pathfinding process. In the first approach, we examined the morphology of growth cone at different regions along the retinofugal pathway. Our result indicates that axons had a pausing behavior during their course of development in the optic chaism. Besides, the growth cone of an axon underwent a morphological change during the pausing period, and the change resulted in the alteration of the direction of growth. In the other two approaches, we tried to analyze the molecular cues involved in the pathfinding process. In one of the approaches, we removed one of the eyeballs in order to examine the effect of the absence of axon-axon interaction. Altogether, three age groups were examined in the monocular enucleation studies and they were embryonic day E14, E15 and E16 embryos. The result showed that reduction of cell bodies for the uncrossed fibers was found in E15 and E16 embryos but not the E14

embryos. This result indicated that the early population of turning fibers were not affected by monocular enucleation but the late population of cells did. The result might also imply that the early and late population of turning fibers relied on different set of guidance cues for their turning process to occur.

Differential PCR display ws used to isolate the differentially expressed genes in different regions of the retina. Seven genes were isolated and three of them were sequenced. One of the DNA fragments was found to have high homology with the gene carnitine Palmitoyltransferase I . The other two DNA fragments were found to be novel genes as there are no high homologous sequence to them in the gene bank. We are going to apply in-situ hybridization to analyze the identity of the cloned genes in the coming future.

Acknowledgments

I would like to thank my supervisor Dr. S.O. Chan for his excellent supervision and his guidance of doing research, both in doing experiment and how to analyze result.

I owe much to the people who provided me technical support. In particular to Dr Alisa Shum and Dr. Thomas Leung. I am indebted to them for their technical help in doing molecular biology and their kindly support in some of the equipment I needed in doing experiment. I would also like to thank Mrs H J Chan-Hou and Mrs Y W Hui-Au for their help when I was doing my research in the Tissue Culture room and in the Histology laboratory and thank Foria Fong for her technical assistance.

Also, I sincerely thank my college Mr. Raymond Li who help me in preparing some of the graphic drawings for my second seminar. Other friends such as Dr. Kwong, Chi, Anny, Amy, Anna, etc. also provided me a lot of support during the period I was working in my laboratory.

Table of Contents

Chapter 1

GENERAL INTRODUCTION

General Introduction

The question of how an axon finds its route to the distant target has been a central issue in understanding the development of the central nervous system. One system which has been extensively studied is the specific axon routing patterns at the chiasm, a major decision point at the ventral diencephalon.

PARTIAL DECUSSATION OF RETINAL AXONS. In early development of mouse embryos, retinal ganglion cells start to appear at dorsocentral retina (Guillery et. al., 1995). Axons of these cells enter the optic chiasm at embryonic day E13.5. These early axons are characterized by thick growth cones as shown by electric mircoscopy (Colello and Guillery, 1992). Once entering the optic chiasm, some of these early axons grow caudally, lateral to a radial glial palisade and enter the ipsilateral optic tract directly (Marcus and Mason , 1995). The late generated axons which dated E15 or later, however, are different from the early axons. Most of these late populations of fibers are crossing fibers, while the remaining axons turn to the same side of the brain. This segregation together with the characteristic

partial decussation pattern at the chiasm, separating uncrossed axons from the crossed axons. This segregation was shown to take place before axons reach the midline of the optic chiasm (Godement et al., 1987b; Colello and Guillery, 1990; Godement et al., 1990; Baker and Reese, 1993; Taylor and Guillery, 1995). Those fibers going to the opposite side of the brain are often referred as crossed fibers while those that turn to the same side of the brain are often referred as uncrossed fibers. This pattern forms a X-shaped pattern of axon pathways known as optic chiasm. The cell bodies of the uncrossed fibers are found mainly located at the ventral temporal retina, namely temporal crescent (Guillery et. al., 1995). However, the cell bodies of the crossed axons spread in all retinal regions.

RETINOTOPICAL ORDER. Another developmental feature of the retinofugal pathway was that the fibers growing into the optic tract from different retinal quadrants were arranged retinotopically in the optic stalk (Colello & Guillery, 1992). However, this order began to lose in the optic stalk by overlapping with one another. The degree of overlapping increased along the optic stalk to the chiasm. Such loss of quadrant-specific order was also observed in developing embryos of rat, cat, monkey and ferret (Horton Greenwood et al., 1979; Naito, 1986, 1989; Baker and Jeffery, 1989; Reese et al, 1994).

Although the retinotopical order is totally lost in the chiasm, another distinct fiber order is established in the developing mouse optic tract. The dorsal axons were found to segregate from the ventral axons, but no obvious segregation of temporal axons from nasal axons. This new fiber order was reported in rats (Chan and Guillery, 1994) and other animals such as ferrets, in which these optic axons have been suggested to come under novel influences as they grow through the chiasmatic region and enter the optic tract (Reese and Baker, 1993; Reese et al., 1994). This pattern of distribution was also found in Xenopus, which indicated that the dorsal-ventral axon segregation was established in the tract before the axons approached their appropriate targets. The actual mechanism of fiber order segregation in different regions of the retinofugal pathway is still unknown. One of the possibility could be the changes in glial environment which might in turn guide the fibers to arrange in different orders.

STUDIES OF GROWTH CONE MORPHOLOGY. To investigate the detail development of the retinofugal pathway, some groups of researchers put their effort in studying the dynamic behavior of axons. In their studies, brain slices were prepared and the dynamic growth behavior of axons were observed using video time-lapse technology (Godement et. al., 1990, Godement et. al., 1994) . Based on their reports, most axons from the ventral temporal retina were crossing fibers in both embryonic date E14 and E15. These crossed axons had simple growth cones,

with an elongated tip and a few short filopodia. Some crossed axons, however, showed a complex morphological change and a pause in their course across the chiasm. For the uncrossed fibers, the uncrossed axons turned at a region 100-200 μm lateral to the midline of the chiasm. These uncrossed axons showed pausing behavior during their growth. During the pause period, there was complicated remodeling of growth cones. Their growth cones had filopodia and lamellopodia initially extended in all directions, with the branch pointing to the ipsilateral tract eventually increased in length while the others retracted. This morphological change finally resulted in a change of growth direction.

GROWTH KINETIC OF RETINAL GANGLION CELL AXONS. About the growth kinetic of retinal ganglion cell axons, the growth rate is quite constant for both crossing and turning axons. The constant growth, however, is interrupted with pausing growth behavior. Actually, it is during this pausing period that the axons undergo morphological change, which lead to alteration of growth direction. It was also reported that the growth cones undergo a long pausing period at the midline of the chiasm. This pausing period may up to several hours. This long period pausing at the midline, however, is still controversial as there was other report showing that growth cones grow directly across the midline of optic chiasm without pausing (Sretavan and Reichardt , 1993) .

STUDIES OF RETINOTECTAL PROJECTION. A lot of information about retinofugal pathway was obtained through studies on non-mammalian vertebrates such as frogs (Holt and Harris, 1983; Holt, 1984; Sakaguchi and Murphey, 1985) and fish (Stuermer, 1988). Evidence showed that positional markers are present in retinal axons and tectal cells (Stahl et al., 1990). Also, interactions between axons mediated by their target cells play important roles in the development of topographic order in retinal projections (Fawcett and O'Leary, 1985).

Evidence from observations of neurons in vitro, in invertebrates, and in the peripheral nervous system of grasshopper in situ, suggested that the shape of growth cones correlated with their behavior (Raper et al., 1983; Argiro et al., 1984). This hypothesis was also supported by Tosney and Landmesser (1985), who reported that an enlarged size and more lamellepodial morphology of motoneuron growth cones in decision region in chick embryos. All these experiments supported the idea that growth cone morphology may be related to the specific cues or interactions with the environment allowing them to respond to specific cues.

CUES FOR PATHFINDING PROCESS. Based on the recent understanding, the possible cues involved in the pathfinding process were hypothesized mainly located at two regions: A) cues located at the retinal ganglion cells and B) cues located at the cell components at the optic chiasm.

A) cues located at the retinal ganglion cells

Retinal ganglion cells could be the sites for the location of cues for the pathfinding process. This idea is supported by the several evidence: 1) absence of pigement epithelium reduces the number of uncrossed fibers and 2) the absence of axon-axon interaction between fibers from the two eyeballs reduces the number of turning fibers.

A.1) CHANGE IN PIGMENTATION OF THE EPITHELIUM AFFECTS PATHFINDING PROCESS. It was reported (Stone et. al. , 1978) that the number of uncrossed fibers in an albino animals was reduced compared with normal pigmented animals. The reduction of cell bodies of the uncrossed fibers could up to 50% of normal for the albinos. This phenomenon of reduction in cell bodies was found in both rat and ferret (Chan and Guillery, 1993) . Other animal models were also used in studying the effect of hyper-pigmentation, such as the Siamese cat (Stone et. al. , 1978). The mechanism of reduction was found to be the reason that the ipsilaterally projected fibers re-routed to the contralateral side (Guillery et al. 1984; Stone et. al., 1978; Chan and Guillery, 1993).

By studying the albino cases using molecular technique, albino mice was found to carry a mutation at the c-locus (Jeffery et. al. ,1994) , which encodes the tyrosinase

gene. Tyrosinase is the key enzyme in melanin synthesis for the retinal pigment. This enzyme produces the cascade of reactions that ultimately results in the production of melanin in the skin and the eyes (Stone et al, 1978) , but it does not produce melanin in other regions of the CNS , such as the substantia nigra. Tissue Culture technique was also applied to study the behavioral difference between the normal and the albino animals by co-culturing explants of chiasm and retina (Marcus et. al., 1996). However, this technique did not find any significant difference between crossed and uncrossed axons from pigmented or albino retinal explants. Both the pigmented and albino retinal explants were found to display the same amount of differential growth when grown on either pigmented or albino chiasm cells.

A.2) AXON-AXON INTERACTION BETWEEN FIBERS OF THE TWO EYEBALLS . Another experiment supported the idea that pathfinding cues could be located at the retina is axon-axon interaction (Guillery et. al., 1995). One approach to study this interaction is using surgical method to remove one of the eyeballs during embryonic day 13. As the axons of the retinal ganglion cells just enter the optic chiasm at E13, removing one of the eyeballs at this stage can eliminate the interaction between axons of the 2 eyeballs. The experiment of prenatal enucleation was done by Chan and Guillery (1993) using rat embryos as animal model. Their result indicated a reduction in the total number of turning fibers.

Similar experiment was also performed in ferret embryos before or during the earliest stages of development of the retinofugal pathway (E23-E26) (Taylor and Guillery, 1995). At the period of E23 to E26, most of the axons that arrived at the optic chiasm were crossing fibers while the uncrossed fibers did not reach this 'decision' point yet. Enucleation at this early stage, again, resulted in a dramatic reduction in the number of uncrossed projection.

All the above experiments demonstrate that there is a requirement for a cell-cell interaction between the axons of the two eyes to establish the normal formation of the uncrossed pathway. However, this hypothesis is still controversial since investigation done by Stretavan and Reichardt (1993), however, showed that no such axon-axon interaction was needed.

Despite the cell-cell interaction between the axons from the two eyeballs, the interaction could be between axons of the retinal ganglion cells and the cells in the environment of the optic chiasm. Based on the studies of developing grasshopper axonal projection, evidence has been given for the existence of intermediate cellular targets that influence axonal trajectories (Bentley and Keshishian, 1982). One of the possible cells involved in the guidance process is the radial glia as suggested by Guillery and Walsh (1987) and Wilson et al. (1988). Similar

suggestion was also provided by the studies in invertebrates (Jacobs and Goodman, 1989).

B) cues located at the cell components in the optic chiasm.

Another possible location for the pathfinding cues is the optic chiasm as there are evidence indicated that 1) the turning fibers never penetrate explants from the optic chiasm and 2) the crossed and uncrossed retinal ganglion cells show different penetration levels to the chiasm cells in in-vitro culture.

B.1) SPECIFIC GROUPS OF CELLS LAY ON THE MIDLINE OF CHIASM. Since it was observed that turning fibers made their turns to the ipsilateral part of the brain before arriving the midline of the optic chiasm, there might be a "barrier" located at the middle part of the optic chiasm. As this unseen barrier could be formed by a group of cells, which can be specifically stained at the midline by immunocytochemistry is a possible candidate of guidance cues.

Several types of antibodies were used to label the group of cells which define a boundary at the midline. Some of the antibodies being used were RC2, SSEA-1, L1 and CD 44. Monoclonal antibody RC2 was a marker for radial glia in embryonic mouse CNS (Reese et al., 1994; Marcus and Mason, 1995; Marcus et al., 1995). This group of radial glia centered around the midline of the optic chiasm and

extended between the floor of the third ventricle and the pial surface of the brain at E12.5. At E15-17, the RC2-labeled cells were found to occupy a more restricted region, approximately 150-200um , along the midline of the optic chiasm. It was reported that growth cones of uncrossed axons did not enter the region occupied RC2-labeled cells. The result indicates that the RC2-positive palisade might help to shape the initial pathway taken by optic axons, creating a region less favorable for optic axon growth. Also, there was group of chiasm neurons stained positively with antibodies against SSEA-1, L1 and CD-44, which formed a structure bordering the posterior edge of retina axons and extended an anterior raphe structure exactly at the midline of chiasm (Marcus and Mason, 1995; Marcus et al., 1995). These chiasm neurons were assumed to be inhibitory to uncrossed axons but not crossed axons. A thin raphe of cells that appeared morphologically distinct from the radial glia was also labelled by free carbohydrate epitope, stage-specific embryonic antigen 1 (SSEA-1). When retinal axons enter the palisade, many axons turned rostrally with respect to the boundary of the SSEA-1-positive cells. Crossed axons did not grow among but were located under the SSEA-1- positive cells. Similarly, an inverted V-shaped neuronal array defining the midline and posterior boundaries of the future optic chiasm were labelled by L1 and CD44(Sretavan et. al. ,1994), where L1 was an immunoglobulin superfamily molecules known to promote retinal axon outgrowth, and CD44, however, was a cell surface molecule that was found to inhibit embryonic retinal axon growth in vitro. By co-culture technique with the retina and chiasm cells, incoming retinal axons did not penetrate this L1/CD44

neuron array, but were turned to establish the characteristic X-shaped optic chiasm along the anterior border of this array .

B.2) THE CROSSED AND UNCROSSED RETINAL GANGLION CELLS SHOW DIFFERENT PENETRATION LEVELS TO THE OPTIC CHIASM IN IN-VITRO CULTURE . The potential interaction between axons from the retinal ganglion cells and the optic chiasm had been studied by in-vitro culture technique. In this approach, explants from dorsal nasal retina and ventral temporal retina were dissected and then co-cultured with optic chiasm on a substrate-coated plate (Wang et. al. , 1995). All those preparations were prepared at E14-E15 when the optic chiasm started to form (Wang et. al. , 1995; Wizenmann et. al. , 1993). These experiments reported that axons from the ventral-temporal explants could not penetrate the cluster of cells formed by the chiasm cells, as if the chiasm cell formed a barrier. However, for the retinal explant from the dorsal nasal retina, the outgrowing axons ignored the chiasm cells and grew straight across the strips.

APPROACH OF INVESTIGATION

Although various approaches were tried to understand the mechanism of pathfinding process in the optic chiasm, the actual issue of the pathfinding process is still not fully addressed. In order to enhance our understanding in the retinofugal pathway, the following experimental approaches were covered:

1. EXAMINATION OF GROWTH BEHAVIOR AND KINETIC. these experimental approach provides a better understanding of the dynamic behavior of axons inside the optic chiasm. As change in growth cone morphology symbolize reading external signals, this study also provide hints about where axons start reading a path guidance signal.
2. INTRA-UTERO ENUCLEATION. Surgical method was used to investigate if there was any immediate change of the number of uncrossed axons after monocular enucleation. These information could resolve the controversy about whether cell-cell interaction between fibers from the two eyeballs was involved in the axonal pathfinding.
3. DIFFERENTIAL PCR DISPLAY. In order to isolate possible cues inside the retinal ganglion cells, the total mRNA from the dorsal nasal retina and the ventral temporal retina was extracted. The pattern of the total cDNAs in these two regions were compared using DNA sequencing gel. Any differentially expressed cDNA in different regions of the retina were extracted from the gel and cloned into a vector named pCR-TRAP. The cloned inserts were further analyzed by both DNA sequencing and in-situ hybridization method.

CHAPTER 2

EXAMINATION OF GROWTH CONE MORPHOLOGY AND DEVELOPMENTAL BEHAVIOR

INTRODUCTION

One of the central tissues in studying the central nervous system is to analyse how axon find their target. One of the system used for this study is the retinofugal pathway. In rodents, the axons of the retinal ganglion cells grow through the optic nerve to the optic chiasm. At the optic chiasm, axons were separated into two groups. One group of the axons cross the midine of the optic chiasm to the other side of the brain while the other group of axons make turn to the same side of the brain. This segregation of axons was found to take place before reaching the midline of the optic chiasm (Godement et al., 1987b; Colello and Guillery, 1990; Godement et al., 1990; Baker and Reese, 1993; Taylor and Guillery, 1995). Various studies tried to address the mechanism of the retinofugal pathfinding process. One of the suggested mechanism is the interaction of axons with cellular elements at the chiasm. This hypothesis is supported by the finding that there are groups of specialized radial glial cells which form a palisade flanking the midline of the chiasm (Reese et al., 1994; Marcus and Mason, 1995; Marcus et al., 1995). The

retinal axons were found to change their course within this zone of radial glial cells (Guillery and Walsh, 1987; Taylor and Guillery, 1994; Marcus et al., 1995). Another possible group of neurons found to be involved in the pathfinding process is the groups stained positively with antibodies against SSEA-1, L1 and CD-44, which formed a structure bordering the posterior edge of retinal axons and extended an anterior raphe structure exactly at the midline of chiasm (Sretavan et al., 1994; Marcus and Mason, 1995; Marcus et al., 1995). It was claimed that these cells exhibited inhibitory effect on the uncrossed fibers to stop them from further advance toward the contralateral side of the brain, as there was evidence that growing axons from temporal, not nasal retina, could grow through strips of membrane from midline of chiasm (Wisenmann et al., 1993). In our study, confocal imaging techniques was used to look at changes in morphology of individual retinal axons and their growth cones in different regions of the chiasm, and to characterize the behaviour of single living retinal axons during the whole pathfinding process across the chiasm.

MATERIALS AND METHODS

Animals

Time mated C57 mice were obtained from the Animal House in the University. The day that the plug was found was designated as embryonic day 0 (E0).

Growth cone morphology in fixed preparation

Four litters of mouse embryos at ages of E13 - E15 were taken out from the mother by Caesarean section. After a brief wash in phosphate buffered saline (PBS), embryos were fixed in 4% paraformaldehyde in 0.1M phosphate buffer for 3 days. A small granule of DiI (1,1'-dioctadecyl-3,3,3',3'-tetramethylindocarbocyanine perchlorate, from Molecular Probes, Eugene, USA) was put through the sclera into either the ventral temporal or dorsal nasal retina (Godement et al., 1987). The embryos were then stored in dark at room temperature in 2% buffered formalin. After 3 weeks, when there is sufficient diffusion of the dye, the retinofugal pathway was dissected, whole mounted on slide, coverslipped and examined under a confocal imaging system (BioRad MRC600 connected to a Zeiss Axiophot photomicroscope), using 514nm line for excitation and a rhodamine filter set for capturing the DiI labelled images.

Individual growth cone labelled by DiI at different regions of the retinofugal pathway were collected using 40x objective (Zeiss Neofluor, N.A. 0.75) and stored in zip disks. Black and white photos of these single growth cones were taken from a high resolution monitor and quantitative analysis of growth cone morphology was done on these prints.

Label of retinal axons in living tissues

Twelve litters of mouse embryos were used in this study. The mothers were killed by cervical dislocation and embryos at age of E14 and E15 were taken out by Caesarean section, and stored temporarily in ice cold DMEM/F12 medium (Gibco, USA). The preparation of the living retinal pathway was similar to the protocol used by Godement et al. (1994). First, a slice of the head containing both eyes, optic stalks, optic chiasm and proximal optic tract was prepared by microdissection in ice chilled serum free medium. A small granule of fluorescent dye DiI was applied to a small region of the retina. In this study, most embryos received a label in the ventral temporal retina, while in others the dye was put into the dorsal nasal retina. The brain slice was then cultured in a 35mm culture dish coated with collagen gel and maintained in DMEM/F12 with 33mM glucose, 15mM HEPES buffer and 10% fetal bovine serum. The culture was kept in an incubator at 37°C. The labels in the slice preparation were checked using a Zeiss Axiophot

microscope with the Rhodamine filter set. Satisfactory labelling of retinal axons was usually obtained 6 hours after application of dye in these preparations.

Confocal imaging of living retinal axons at the chiasm

The brain slice preparation of the retinofugal pathway was imaged under a modified confocal imaging system connected to a Zeiss Axiophot microscope. During the recording period, the brain slice was maintained at 37°C with a heated mounting stage and with a continuous flow of culture medium. The optic stalk and chiasm, especially the midline, was recognized in these preparations with phase contrast optics. DiI labelled axons were excited with the 514nm line emitted from the argon ion laser (25mV) and the emission signal was collected with an enhanced photomultiplier detector. The laser dose was reduced to 1% using neutral density filter in order to minimize possible photodamage to the labelled axons. Series of optical sections were taken through different focal planes in the chiasm and the images were stacked using the COMOS software to produce a projection image of the labelled axons. This technique enabled us to analye growth of a number of axons simultaneously in a single preparation. The labelled retinal axons in this preparation could usually be maintained and recorded for 4 hours, showing smooth axon profiles and continuous growth. After this time window, the labelled axons started to show signs of degeneration, which was manifested by appearance of beaded profiles, retardation or even stop in all axonal growth. The recording was

usually finished in 3 hours, except in some cases the brain slice was imaged up to 4 hours. Most time-lapsed confocal images were taken at a defined interval, usually 15 minutes, using a 10x (Zeiss Neofluor, N.A. 0.3) or a 20x (Zeiss Neofluor, N.A. 0.5) objective. Some growing axons were imaged using a 40x objective. However, these axons usually started to degenerate after one hour in recording, possibly because of the photodamage effect of the laser beam under such a high magnification. These time-lapse images were stored in either a magneto-optical disk (Sony, Japan) or a Iomega zip disk.

The growth kinetic and behaviour of these labelled retinal axons were analyzed on drawings of the axons. The axon morphology was copied either directly from the monitor or from color prints of confocal images. The growth distance of a particular axon was measured as the distance travelled by a growth cone in drawings of two consecutive confocal images recorded within a defined time interval.

RESULTS

Axonal outgrowth in the retinofugal pathway of mouse embryos

The study of the axonal outgrowth was done using fixed mouse embryos with the age ranged from E13 to E15. Axons were labelled by fluorescent dye DiI which was put at the ventral temporal retina where most of the cell bodies of the uncrossed fibers located (Godement et al., 1987). In the animal model we used, the axon first arrived the optic chiasm at E13. At this early period, most of the fibres are crossing fibers (Godement et al., 1987), with only a few axons turn to the ipsilateral part of the brain. The number of uncrossed fibers increases at E14 and E15. A confocal diagram showing the turning fibers at the optic chiasm at the optic chiasm at E15 was done at figure 1.1A and 1.1B. It was noted at figure 1.1b that all the turnings occur at a position before 100um from the midline of the optic chiasm. These turning axons were characterized by the presence of backwardly pointing processes. Also, this region before the midline of the optic chiasm was denoted as pre-midline region while the region beyond the midline of the optic chiasm was denoted as post-midline region.

Remodeling of growth cone morphology during pause periods

About 50 growing reintal axons were studied in this part and 26 of these axons were taken for quantitative analysis for their growth behavior and kinetic during their development at the optic chiasm. These axons were grouped according to their position at the optic chiasm and were classified to pre-midline and post-midline axons. Altogether, there were 12 axons being imaged at the pre-midline region while there were 14 axons imaged at the post-midline region.

Based on our observation, axons, both at the pre-midline and post-midline region, exhibited pausing behavior. During this pausing period, the axons had their growth cone morphologies change. One of the examples images were shown in figure 1.2. In this figure, an axon was approaching the midline of the optic chiasm during the time of recording. This axon exhibit a constant grow during the period from the time of 0 minute to 60 minute. At the time of 85 to 140, when the axon was close to the midline of the optic chiasm, it did not show obvious advancing. During this pausing period, this axon had branching of its growth cone ocurred. One side of the processes was retracted while the other side of the growth cones continued to extend. This morphological change end up with changing in the direction of growth. Such advance and pause cycles were also seen in axons that grew in other regions of the chiasm.

Axon growth at the pre-midline region

The major characteristic for axons at the pre-midline region is that axons were segregated into crossing and turning fibers. Figure 1.3 is diagramatic presentation of a series of confocal micrographs. Most of the axons exhibited a simple growth cone and had a smooth profile of growth. One characteristic of axon growth in the premidline chiasm is that each axon had its own tempo of growth. For example, while axon 'A' advanced steadily in the recording period, axons 'C' and 'D' had no obvious increase in length from 0 minute to 80 minute in recording. However, a dramatic increase in length of axon D was observed in the following 20 minutes while axon 'C' was still pausing. Another phenomenon for these pre-midline axons was that the turning fibers had their growth cone remodeling more extensive than the crossing fibers. The axon B in figure 1.3 is an example showing this phenomenon. This axon turned at the lateral region of chiasm, 350μm away from the midline. This axon displayed initially two short appendages from the axon terminal. The appendage pointing towards the midline gradually retracted at 30 min and the one that pointed to the ipsilateral tract after a pause for 100 minutes started to grow to the ipsilateral optic tract. Within this pausing period, the growth cone underwent a dynamic modification of its shape which eventually led to its turning.

Axon behaviour at the post-midline region

Figure 1.4 shows a typical example of axons at the midline and post-midline region in E15 embryos. Axons at the post-midine region were characterized by larger in the size of growth cone and more processes. Also, these axons kept on changing their direction of growth. For example, the fascicles labelled A, B and C were three separated fascicles at time 0. However, starting from time 110min, these fascicles started to spread away and, eventually, fascicles A and B met each other at time 215 min.

Growth dynamic of retinal axons at the chiasm

The growth dynamic of 23 individual retinal axons were analysized (Fig 1.5). Of all these axons, 12 of them were located at the premidline region while 11 of them are located at the post-midline region. Each plot represents one single axon being analyzed, with their distance of growth against the period of recording. Based on the graphs, axons exhibit a continuous growth during the whole recording period. However, their growth are interrupted by pausing behavior (zero displacement in the curves) or retractions of their growth cones retractions (negative displacements). The events of interruption were indicated by small arrow heads on the graph. These pausing periods last around 15-30 minutes and were observed in

axons at both pre-midline and post-midline chiasm. The growth rates of these axons were calculated by measuring their slopes of growth curves and the results are summarized in Table 1.1. Based on the analyzed result, the growth rates of the axons in pre-midline region are similar to the growth rates at the post-midline region, ranging from 0.2 to 0.8 μm/min i.e. 12 - 48 μm/hr or 0.288 - 1.152 mm/day. The average growth rate was 0.50 ± 0.05 μm/min and 0.52 ± 0.06 μm/min in the pre-midline and post-midline chiasm, respectively. Also, there was no significant difference between growth rates of retinal axons at these two regions ($p>0.05$ by student T-test).

DISCUSSION

GENERAL OBSERVATION. In this study, we have investigated the growth behavior of retinal axons at different regions of the optic chiasm in E14 and E15 mouse embryos. The axonal growth behavior was studied using both living and fixed preparation. The living preparation has the advantage that it allows us to view the growth of axons in real time so that we can have a better understanding about the whole process of turing. For the fixed preparation, they can tolerate a higher dosage of laser used in confocal microscopy than the living tissue. As such, a high magnification and high resolutions were obtained. The areas being studied include the pre-midline, midline and post-midline regions of the chiasm. Our studies also obtained information about the nature of turning at the optic chiasm. For example, uncrossed axons were found to turn at a range from 100um to 200um relative to the midline. This information provides us the hint that the molecular cues for the turning process might flank the midline of the optic chiasm, instead of restricted to a narrow region. As all the turning processes occur before reaching the midline of the optic chiasm, it may be possible that there is a middle barrier located at the center of the optic chiasm which prevents the uncrossed fibers to pass through the midline. However, there is no indication that the cues for turning of uncrossed fibers belong to the midline barrier. As the precision of the retinofugal pattern in

the optic chiasm is important, the existence of the midline barrier may be crucial to ensure that no uncrossed fibers made turn after passing through the midline of the optic chiasm.

Behaviour of living growth cones at the chiasm

For the studies of the growth kinetic, It is found that the growth rate of retinal axon at the chiasm has a range, from about 0.23 to 0.83 um/min. However, there is no significant difference between the growth rate at the pre-midline region and the post-midline region.

PAUSING BEHAVIOUR. The growth behavior of the axons in chiasm is characterized by a pattern of intermittent advance interrupted with periods of pause and sometimes retractions. These phenomena are observed in all regions of the chiasm. The result is consistent with the studies by other groups of researchers(Godement et al., 1994; Wang and Mason, 1997; Sretavan and Reichardt, 1993).

The nature of the pausing phenomenon is still unknown but there is evidence supporting the idea that mechanism is included in the pathfinding process. Since axons from all parts of the retina are intermixed at the chiasm (Chan and Guillery, 1994), active mechanism must be involved in the pathfinding process to sort out the uncrossed fibers from the crossed fibers. It is hypothesized that the guidance processes are probably mediated through interactions of retinal axons, cellular elements within the chiasm, and molecules in the extracellular matrix. The fact that axons exhibit pausing behavior could also be co-related to the active mechanism as it is possible that the axons needed to slow down for reading external signals.

GUIDANCE CUES. Currently, there are no ideas about what the extracellular signals could be involved in the pathfinding process. Still, various studies provided some hints of this tissue. First, electron microscopic studies of chiasm in mouse embryos revealed that retinal axons are in close contact with profiles of radial glia and other neurites (Bovolenta and Mason, 1987; Marcus et al., 1995). Second, changes in growth direction of retinal axons are always associated with an alteration of glia environment, such as the reshuffling of retinal axons at the juncture of optic nerve and ventral diencephalon where there is a change from interfascicular glia to radial glia (Guillery and Walsh, 1987; Colleo and Guillery, 1992; Reese et al., 1994). Third, if the CD44 immunoreactive chiasm neurons were ablated before any retinal axon outgrowth, the retinal axons in subsequent

development are unable to grow into the chiasm (Sretavan et al., 1995). These findings lead to the suggestion that axon guidance in the chiasm depends at least in part on interactions with the cellular context resident in the chiasm.

CHAPTER 3

STUDY BINOCULAR INTERACTION BY INTRA-UTERO ENUCLEATION

Introduction

During the development of the retinofugal pathway, the uncrossed fibers make turns before reaching the midline of the optic chiasm. This turning process seems to require the presence of the crossing fibers from the opposite eye as there were reports that the removal of one of the mouse eyeballs resulted in a reduction of the number of uncrossed fibers (Godement et al., 1987b, 1990). Similar result was also obtained using ferret as animal model (Guillery, 1989). The monocular enucleation studies were further supported by the subsequent studies (Chan and Guillery, 1993; Taylor and Guillery, 1995) who showed that monocular enucleation done in an earlier age could further reduce the number of uncrossed fibers. All these results demonstrate that fiber-fiber interactions between the two eyeballs are needed for the axonal pathfinding process.

However, the report given by the group Stretavan and Reichardt (1993) showed a contradictory result which indicated that monocular enucleation did not reduce the number of uncrossed fibers.

The cause of the conflict between the separated results is still unknown. However, there are reports showing that a wave of cell death occurs to the prenatal neuronal

cells (Jeffery, 1984; Linden and Serfaty, 1985; Chan et al., 1989). As the group of fibers being studied by Sretavan and Reichardt (1993) could be the early population of cells, it is possible that the event of prenatal cell death could be the reason causing the contradictory results. In order to clarify whether an early removal of fiber interaction at the chiasm has a direct effect on the development of the uncrossed component of the remaining eye, we tried to address the immediate effect of the monocular enucleation to the C57 mice embryos by studying the cell number of uncrossed fibers at E14, E15 and E16. I also analyzed the result of different age groups by dividing the cells into the temporal crescent (TC) and the nasal retina (NA) in order to check the impact of monocular enucleation on the pathfinding.

Materials and Methods

Time-mated C57 mice were obatined from the Animal House in the Faculty of Medicine. The date that a vaginal plug is found is denoted as embryonic day 0 (E0). The monocular enucleation surgery was done on E13 embryos. Pregnant mice were anaesthetized with a mixture of hypnorm(Jenssen Animal Health, English) and hynovel (Roche, Switzerland) (1:1 in 2 parts of distilled water) (0.1 ml/10g body weight). The pigmented eyeballs in embryos were readily identified through the thin uterine wall. A small opening was made above an eye and the eye was then moved either by fine jeweler forceps or by a micro-cauterizer. Only one embryo was operated on each uterine horn. The wound on uterine wall was closed by 7.0 surgical suture, in which the abdominal muscles and a skin wound were sutured separately. The mother was then allowed to be recovered in a warmed environment. The operated embryos were taken out from the mother 1 day to 3 days after surgery. The unoperated siblings within the same litter served as controls. The mothers were killed by cervical dislocation and embryos were collected immediately in chilled phosphate buffered saline (PBS) by Caesarean section. The embryonic membranes were removed and embryos were decapitated. The heads were then fixed in 4% paraformaldehyde in PBS at 4°C. After 3 days, the heads were embedded in a mixture of gelatin-albumen and sectioned horizontally on a vibratome. At a level about 400-600 um above the chiasm, the optic tract was

identified in the horizontal section of the brain as a discrete fiber bundle located at the lateral diencephalon. Several granules of a fluorescent dye, DiI (Moleculars Probes, Eugene USA), were inserted into the optic tract, on the left in controls, and on the side ipsilateral to the remaining eye in enucleates, to label all retinal axons at this level. The labelled embryos were then kept in dark at room temperature in 2% buffered formalin.

After 6 to 12 weeks, depending on the age of embryos, retinas were dissected out in PBS and flat-mounted on glass slide. A cut was made in the dorsal pole of the retina before removing the eyeball in order to mark the orientation in later observation. The retina was mounted in an antifading medium containing 0.5% p-phenylene-diamine and coverslipped. Retrogradely labelled retinal ganglion cells were examined under a fluorescent microscope (Zeiss Axiophot photomircoscope). Black and white negatives (Ilford 400) were taken consecutively through while the retina ipsilateral to the labelled tract using a 10x objective. The number of ipsilaterally projecting retinal ganglion cells was later counted on a montage of these prints. The cell counts were made separately in two regions of the retina, namely temporal crescent and nasal retina. In adult retina, most retinal ganglion cells that have an uncrossed axon are located in peripheral regions of ventral temporal retina, forming the temporal crescent. Only a few ipsilateral cells are found in the nasal retina. Labelled cells in the retinas contralateral to the labelled tract were photographed using a 5x objective. The cell counts in the control and experimental animals were analyzed using Mann-Whitney non-parametric tests.

Results

ANATOMICAL STRUCTURE AFTER SURGERY. In this study, the monocular enucleation was done at the E13 embryos. During this time period, the early group of nerve fibers has just arrived the optic chiasm. As it was important that the surgical method should not cause any problem to the embryos, dissection of the embryos after surgery was used to examine the completeness of the eye removal. As shown in Figure 2.1A, the monocular enucleated embryos do not show any significant morphological change except the absence of one of the eyeballs. One of the samples demonstrating a horizontal dissection of an E16 embryos is shown in figure 2.1B and 2.1C. These figures showed that the the optic stalk was absent in the monocular enucleated embryos.

CONTROL GROUP. Another concern need to be counted in the experiment of monocular enucleation was whether the retinal ganglion cells were fully labelled or not. In order to ensure that all the uncrossed fibers were labelled, we used the contralateral eyeball as a positive control. Since the cell bodies of the crossed fibers located all over the retina, a full labelling had to give an entirely labelled contralateral retina. Figure 2.2A and 2.2B showed retinal labels after DiI labelling.

Uncrossed retinofugal pathway in normal embryos

THREE AGE GROUPS. The ages of the embryos studied by us include E14, E15 and E16. In E14 embryos, the cell bodies of the uncrossed fibers located mainly in the central part of the retina as shown in figure 2.3A. In the subsequent development, the number of ucrossed fibers increased (figure. 2.3B). Also, there are increasing concentration of cell bodies of uncrossed fibers in the region of temporal crescent, especially at E16 embryos(Fig. 2.3c). The sequence of development of uncrossed pathway is in accordance with the findings reported in an earlier study of mouse retinofugal pathway (Colello and Guillery, 1990).

SUBTYPES. The three age groups E14, E15 and E16 embryos are further classified into the two subtypes and they are (1) the control and (2) the monocular enucleated embryos. For the retinas in each subtype, they are divided into two different regions: the temporal crescent (TC) and the nasal retina (NA). The reason of dividing the retina into these two regions is that the locations of cell bodies of the early uncrossed fibers (E14 embryos) are spreading among the whole retina. For the late uncrossed fibers (E16 embryos), these cell bodies mainly located at the temporal crescent region of the retina. As a result, retina divided into the TC and the NA region allowing studying the effect of monocular enucleation to these two groups of uncrossed fibers separately. The definition of the temporal cresecent

region from the nasal retina is based on the following criteria: First, the orientation of the temporal crescent region is at the ventral temporal part of the retina; second, the temporal cresecent is restricted to the peripheral part of the retina but not the central part of the retina; third, border of the temporal crescent is featured by a vague sudden increase in the cell numbers of the uncrossed fibers.

Immediate effect of early monocular enucleation on uncrossed retinal pathway

The immediate effect of monocular enucleation in the surgically treated embryos and the control group was examined using DiI labelling and the number of labelled cell bodies was counted. In E14, those cell bodies of the uncrossed fibers mainly located at the central region of the retina (Fig. 2.4). Statistical test using Mann-Whitney non-parametric tests did not show any significant difference in cell number between the monocular enucleated group and the control group ($p > 0.05$) (Table 2.1).

In most E15 control embryos (5 in 7), labelled cells were first found in the ventral temporal retina (Fig.2.5). It was noted that enucleation cause significant reduction in the number of cell bodies of the uncrossed fibers at temporal crescent but not those cell bodies in the nasal retina.

The reduction of cell bodies of the uncrossed fibres was further enhanced in E16 embryos ($P<0.001$), at which the concentration of the cell bodies at the ventral temporal was very obvious (Fig.2.6). This reduction of cell bodies is contributed

mainly by decreasing the cell bodies number in the temporal crescent region ($p<0.01$) but not those cell bodies at the nasal retina ($p>0.1$).

Discussion

In the present study, we demonstrated that early enucleation of the retina led to a reduction of the cell bodies of uncrossed fibers. The reduction was especially significant for those cell bodies located at the ventral temporal crescent of the retina compared with those cell bodies located at nasal part of the retina.

Early population of uncrossed fibers

In adult retina, the cell bodies of the uncrossed fibers are located at the ventral temporal crescent of the retina as shown by those studies on rodent (Jeffery and Perry, 1982; Godement et al., 1987b; Chan and Jen, 1988). Only a few of cell bodies are located at other part of the retina. However, in the early embryo, the cell bodies of the uncrossed fibers are mainly located at the central part of the retina (Godement et al., 1987b; Colello and Guillery, 1990). These populations of early cell bodies located at the central part of the retina could represent a developmental error commonly found in the initial phase of pathway formation. The error is reported to be corrected by post-natal cell death which acts to refine the retinal terminations within the targets (Jeffery, 1984; O'Leary et al., 1986; Chan et al., 1989; Nakamura and O' Leary, 1989).

Axon guidance of uncrossed axons depends on the presence of fiber from the other eye

The result in this experiment indicates clearly that the number of cell bodies for the uncrossed fibers relies on the co-existence of the two eyeballs. It is especially the cell bodies which located at the ventral temporal crescent of the retina that had significant reduction in the number of cell bodies after removal of one of the eyeballs. The result is consistent with the previous studies (Godement et al., 1987a and 1990; Chan and Guillery, 1993; Taylor and Guillery, 1995)

SUGGESTED AXONAL GUIDANCE CUES. Based on the above findings, a determinant for the axonal pathfinding process might exist at the ventral temporal crescent. This determinant could be a surface property different from the cells in the nasal part of the retina (Guillery, 1992; Chan and Guillery, 1993; Taylor and Guillery, 1995). This cell surface property is important for them to decide whether they should turn to the same side or cross to the other side of the brain when they encounter the local guidance cues at the optic chiasm. The nature of this axonal guidance cue at the retina is still unknown. However, this cue may be related to the ocular pigment as the number of uncrossed fibers reduced in albino animals which do not have ocular pigment (La Vail et al., 1978; Guillery et al 1984; Guillery et al., 1987).

Moreover, two more determinants at the chiasm are required for the proper axon turning. These two determinants have effects on the uncrossed fibers but not the crossed fibers. One of these signals is responsible for stopping the further advance of the uncrossed fibers and it could be the reason why all the turning processes occur at the pre-midline region of the chiasm. The other signal guides the uncrossed fibers to find their way to the ipsilateral part of the brain. For the signals which pause the advance of the fibers, they are likely to be the cells inside the optic chiasm. One example is the glial cells which form a palisade straddling the midline of the chiasm (Marcus and Mason, 1995; Marcus et al., 1995) when the first retinal axon enters the chiasm. Another possible type of cells is the chiasm neurons that express both SSEA-1 and CD44 (Sretavan et al., 1994; Marcus et al., 1995). Elimination of the CD44 positive neurons in the chiasm resulted in an inability of retinal axons to grow into the chiasm (Sretavan et al., 1995).

Another signal for the axonal pathfinding process is the selective fasciculation with crossed axons at the chiasm. Disruption of this signal after an early removal of one of the eyeballs resulted in an immediately reduction of the uncrossed component. However, the reduction level is time dependent. Enucleation at a earlier stage of development caused a more obvious reduction of uncrossed componenet (Chan and Guillery, 1993; Taylor and Guillery, 1995).

Unlike the cells in the ventral temporal crescent of the retina, the uncrossed components with their cell bodies located at the central part of the retina are not affected by the monocular enucleation. This group of axons may find their route on

a random basis at the chiasm, without requiring any specific guidance cues as the late uncrossed components from the ventral temporal crescent of the retina. It is suggested that these axons act as pioneer to guide late developed uncrossed axons (Sretavan, 1990) but there is still no firm evidence to support the current idea.

CHAPTER 4

ISOLATION OF DIFFERENTIALLY EXPRESSED mRNA IN DIFFERENT REGIONS OF THE RETINA

Introduction

Based on current studies, the pathfinding process at the optic chiasm is controlled by a local signal at the optic chiasm which let the crossed fibers to cross the midline of the optic chiasm while instructs the uncrossed fibers to turn to the same side of the brain (Godement et al., 1990; Sretavan, 1990; Sretavan and Reichardt, 1993; Godement et al., 1994). It is suggested that this local signal is inhibitory to the uncrossed fibers but permissive to the crossing fibers (Godement et al., 1990; Wizenmann et al., 1993) and the location of this local cue may be at the midline of the optic chiasm (Marcus et al., 1995).

The location of another possible cue for the pathfinding is the retina. The fact that the cell bodies of the uncrossed fibers mainly located at the ventral temporal crescent (fig 3.1), while their nerve fibers intermingle with those fibers from the nasal retina at the optic chiasm has already indicated that there are different instrinic properties in the cell bodies of the crossed and uncrossed fibers (Colello and Guillery, 1990 ; Chan et al., 1993). There are three criteria to be noted for the

different instrinsic property in retinal ganglion cells: First, as the cell bodies of the uncrossed fibers located at the peripheral part of the retina while the cell bodies of the crossed fibers at the nasal part of the retina, the signal should exist with a concentration gradient from the ventral temporal region to the nasal region of the retina. Second, expression of this cue must be around the time before or when the axons reach the midline of the retina. Finally, expression should be affected by the ocular pigment since the number of uncrossed fibers is significantly reduced for the albino animals which have a deficiency in ocular pigment production.

POTENTIAL CANDIDATE GENE. Several proteins and genes were reported to be included in the pathfinding process in mouse and chick (Trisler et al., 1981; Rabacchi et al., 1990; McLoon, 1991; Deitcher et al., 1994). The actual function of these proteins or genes could be related to defining the development of retinotopic maps or related to the determination of specific cell type across the retinal layers (Pachnis et al., 1993; Liu et al., 1994).

One of the molecules under studies in the guidance of axonal path in the optic chiasm is the GAP-43. GAP-43 is the growth-associated protein. It is localized to the internal surface of the growth cone membrane and is expressed at a high level in neuronal growth cones during development and during axonal regeneration. In a recent study done by Stephen et. al. (1995), the GAP-43 deficient mouse was used as an animal model and it was found that the axons were trapped in the chiasm in

the mice at E15 to P2, without processes that grow across the optic chiasm or make turn to the same side of the brain. The trapped axons, however, continued their journeys in the subsequent weeks of life by entering the optic tract. The adult central nervous system of the mice was anatomically normal. However, there is an unusual large number of fibers continued to be misrouted to the contralateral optic nerve.

OTHER ANIMAL MODEL. Apart from mammals, insects are another model used for the study of pathfinding process. One of the molecules found in the axonal guidance process of insects is the semaphorin. Semaphorins comprise a family of cell surface and secreted proteins that are conserved from insects to human . These molecule were reported to be the diffusible axonal guidance cue for patterning sensory projection by selectively repelling axons that normally terminate dorsally. Other members of the semaphorins, for example, the Sema I, are transmembrane protein that has been implicated in guiding pioneer axons in the grasshopper limb bud. In human beings, similar molecule has been found and the corresponding name is H-Sema III.

In the animal model like Drosophila, a protein named Fasciclin III was found to be involved in the pathfinding process. Fascilin III is a cell adhesion molecule of the immunoglobulin superfamily and is expressed by motor neuron RP33 and particular muscle cells at which the molecules specifically target. Mutation in these

molecules resulted in innervation of axons at non-target cells so that these molecules were postulated to be the path guidance molecules.

The present study is to investigate the molecular cues involved in the pathfinding process by looking for genes that are differentially expressed in the retina. Here we present some genes which were differentially expressed in the retina. In order to search for these intrinsic cues in the retina, the differential PCR display was used. The differential expressed genes shown by the differential PCR display were then extracted and cloned into a vector named pCR-TRAP. The cloned PCR products were further analyzed by both DNA sequencing method and the in-situ hybridization technique. Through DNA sequencing, the cloned gene sequences were obtained and checked through the gene bank to get more background information about the insert. Through in-situ hybridization, the expression position of the clone inserts can be visualized to check whether the gene was differentially expressed at the retina.

Materials and Methods

Differential PCR display:

C57 mice were used in this study. The females were time mated in the Animal House of Medical Faculty and kept until the embryoswere at embryonic day 13 (E13).

Dissection of retina

The pregnant mice were killed by cervical dislocation and embryos were taken out using Caesarean section. In this study, 30 mouse embryos were used. The retina was dissection in ice cold DMEM-F12 medium (Gibco, Life Technologies, USA). Before dissecting out the retina, a cut was made at the dorsal nasal pole of the eyeball to mark the orientation. The cornea, lens and vasculature on the inner surface of the retina were removed using jeweller fine forceps. The retina was then dissected out and bisected roughly at the central border of the presumptive temporal crescent. The retinal tissues were immersed immediately in a lysis buffer which provides a high salt and denaturing condition to inactivate RNases and ensure isolation of intact RNA.

Extraction of total RNA from retinas

The retinal tissues in the lysis buffer were homogenized using a QIAShredder kit (Qiagen, USA). Total RNA in the lysates was isolated using the RNeasy kit from Qiagen, which utilizes the specific binding properties of silica gel-based membrane for purifying RNA. The eluted solutions were treated with DNaseI to remove contaminated chromosomal DNA (MessageClean kit, Qiagen). The amount of total RNA was then measured by spectrophotometry. In this study, we obtained about 7 ug total RNA from the nasal retina and 3.6ug from the temporal retina.

Differential display of genes from retina

Genes that are expressed differentially in either temporal or nasal retina are identified using the differential display technology developed by Pardee and Liang (Liang and Pardee, 1992). Messenger RNA in the highly purified total RNA was reversely transcribed with oligo-dT primers anchored to the beginning of the poly(A) tail (in RNAimage kit 1, GenHunter Co, USA), followed by polymerase chain reaction (PCR) in the presence of a second arbitrary primer (13 bases in length) and radioactive nucleotide (α-[^{35}S] dATP, Amersham, HK). By using specific combinations of oligo-dT and arbitrary primers, a specific subpopulation of mRNA was amplified. These cDNA fragments were then separated on a DNA

sequencing gel (6% polyacrylamide gel, Sigma Chem, USA). The seqeuencing gel was dried, transferred to a Whatman No.1 membrane and exposed on an X-Ray film (hyperFilm-MP, Amersham, UK) in dark for 3 days. The film was exposed using a Kodak automatic film processor. Bands that were identified only in one retinal region but not the other were marked and cut out from the dried membrane. The cDNA fragments of these presumptive differentially expressed genes were extracted using the QIAEX II kit (Qiagen, USA) and collected in distilled water. They were reamplified by PCR (30 cycles) using specific pairs of 5' arbitrary and 3' oligo-dT primers in order to accumulate enough amount of cDNA for later cloning process.

Condition for the PCR reaction

The PCR condition for the PCR reaction was pre-heating at 94°C, 2min; denaturation at 94°C for 30 seconds; annealing at 52°C, 40 seconds; elongation at 72°C, 1 minute; extra-elongation at the last time at 72°C, 5 minutes. After the PCR reaction, the inserts were further analyzed by the DNA sequencing method and also in-situ hybridization and the result was shown in the following sessions.

Cloning of differentially expressed genes in retina

The amplified sequences of the identified cDNA were cloned into a plasmid vector pCR-TRAP (GenHunter, USA). The insertion of PCR fragement into the multiple cloning site in this plasmid disrupts production of a repressor gene, thus releases the suppression of tetracycline resistance gene in the downstream sequence. The vector together with the inserts was transformed into a GH competent E.coli cells and inoculated on a LB agar plate containing tetracycline (Life Technologies, USA). The bacterial colonies were then picked and maintained in LB broth.

In order to check whether cloned vectors contain insert of the right length that had been identified in the differential display, a miniprep of the plasmid was done using a QIAprep Spin Plasmid kit (Qiagen, USA). This protocol yielded up to 20ug plasmid DNA from 1-5ml overnight cultures of E.coli in LB mdium.

The cloned inserts were checked by PCR method using the purified plasmids that contain the cDNA of interest, and a pair of primers (Rgh and Lgh) at both sides of the insert. The presence of inserts and their sizes were determined by running the PCR products on 1.5% agarose gel.

Sequencing the cloned idfferentially expressed genes isolated from retina

The cloned inserts were amplified by PCR reactions using the Lgh and Rgh primers. The PCR products were then purified and ready for the sequencing reaction. The purified PCR products that served as templates for the sequencing reaction using product were then fed into an automatic sequencer (ABI Prism 310, Perkin-Elmer Co., USA) for generating the sequences of our inserts.

The identified sequences were compared with the known sequences in the GenBank via the internet (http://www3.ncbi.nlm.nih.gov/BLAST/nph-blast) to determine whether the isolated genes were novel or in high homology to other known genes.

Results :

In order to collect enough retina samples for the experiment of differential PCR display, 30 retinas were dissected in mouse embryos. About 7ug of RNA were extracted from the nasal retina and 3.6ug RNA was isolated from the temporal retina. The RNAs were reversely transcribed to cDNA by a single base anchored oligo-dT primer in 3' terminal and a 13-mer arbitrary primer on the 5' terminal. The cDNAs were then separated by DNA sequencing gel. In each pair of lanes, which corresponds to the nasal and the temporal retina, shows a matching in

expression bands in overall but there were some bands which were differentially found in one part of the retina but not the others. Figure 3.2 shows one of these examples with two PCR fragments found exclusively in the temporal but not the nasal retina. These bands were pinned at both ends on the X-ray film under which the dried gel was aligned precisely with reference to marks made before the exposure.

Reamplication and cloning

There were altogether eleven bands extracted and amplified using specific pairs of primers. Of all the eleven bands, 6 of them are successfully reamplified. These cDNA fragments have their size range from 100 to 280 base pairs (Fig. 3.3). The cDNA fragments were then cloned into pCR-TRAP vector. Analysis of the presence of cloned cDNA were done by PCR reaction using purified PCR products and a primer set (Rgh and Lgh). The length of the amplified DNA fragments was found by comparing it with the DNA marker and the result is shown in Table 3.1. Since the clones TA4.1, TA8.1 and NC2.1 have lengths matching the size of the insert from the previous DNA sequencing gel, they were taken for subsequent analysis.

Sequences of the identified genes

Around the three cloned genes, TA4.1 and TA8.1 are bands expressed only in the ventral temporal retina while sample NC2.1 corresponds to the band for the nasal retina. The sequences of these three genes were shown in figure 3.4.
To verify these genes, the following criteria were applied: first, the genes must contain poly-A tail in order to confirm that their sources are mRNA; second, as the primer sets for the differential PCR display contain HindIII restriction sites (AAGCTT), the insert must contain the cutting sites at their flanking sequences.

The sequences of the three genes were checked through the GenBank. The GenBank then returned the result of the corresponding gene information based on the homology matching of their base pairs. Based on the searched result, C.elegans cosmid C54D10 gave the highest matching with sample 1 (clone TA4.1). 59 out of 82 bases were matched (approximately 72% matching). Sample 2 (clone TA8.1) has 87.2% matching with the gene sequence of carnitine palmitoyltransferase I in rats. Sample 3 (clone NC2.1), C.elegans cosmid RO6C7 give the highest percentage of matching (75.4%). Another gene shows high percentage matching to sample 3 is the GABA-A receptor alpha-5 subunit gene (42.6%). The alpha 5 subunit of the GABA-A receptor was reported to be expressed in a few brain areas such as cerebral cortex, hippocampal formation and olfactory bulb granular layer, as shown by in situ hybridization histochemistry.

Discussion

This report shows the preliminary study in using the molecular approach to isolate the molecular cues included in the pathfinding process in different parts of the retina. By using the differential PCR display, PCR and cloning method, three different genes were isolated and cloned. These genes were sequenced and the searched results using GenBank show a certain degree of homology to some currently known genes.

Genes that are expressed in the developing retina

Several groups of genes were reported to be involved in the embryonic development. They can be classified into three different categories in accordance with their temporal and spatial differences in expression. The first group of genes is responsible for the morphogenesis of retina and is expressed in the whole retina. Examples of this type of gene include the small eye gene (Pax6) in the mouse (Walther and Gruss, 1991) and its homolog eyeless (ey) in Drosophila (Quiring et al., 1994). These paired box-containing genes function as transcription regulators during the eye morphogenesis. Mutation of the Pax6 genes results in eye malformation such as small eye syndrome in mouse and Aniridia in human (Hill et al., 1991; Tan et al., 1991). Another paired box gene Rx, which was originally isolated in Xenopus embryos and later found in zebrafish, mouse, drosophila and

human, also had a crucial function on controlling the eye development (Mathers et al., 1997). Mouse embryos that have a null allele of this gene do not form the optic cup and so do not develop an eye. This gene appears to be included in both vertebrate and invertebrate.

The second group of genes determines the cell fates in the retina. It was expressed in specific laminae and cell types in the developing retina. One of the examples of this type of genes includes the homeobox gene Chx10 which is expressed in the inner nuclear layer of mouse retina (Liu et al., 1994). Another example is a proto-oncogene c-ret (Pachnis et al., 1993). This gene is expressed in the ganglion cells, amacrine cells and horizontal cells in the postnatal mouse retina.

The third group of genes has a topographic difference in expression within the developing retina. Example is the TOP molecule that is expressed 35 fold more in the dorsal than ventral retina in chick embryos (Trisler et al., 1981). Another example is the enzyme aldehyde dehydrogenase which expressed mainly in the dorsal part of the mouse embryo retina (McCaffery et al., 1991). This enzyme functions at oxidizing retinaldehyde to retinoic acid.

Molecules that show a differential expression in the nasal temporal axis of retina were reported in chicks and mice. A temporal retinal axon protein (TRAP) was shown to express exclusively in the temporal hemiretina in the chick (McLoon, 1991). This molecule may play a role in patterning the nasal-temporal axis in the retina. Besides, two winged helix genes, BF-1 and BF-2 marked the nasal and

temporal hemiretinas respectively during the early development of this visual organ (Hatini et al., 1994).

Results of these studies provided evidences that these topographic specific genes are related to the formation of precise retinotopic termination in the primary visual targets. However, these genes are not likely to be included in the development of partial decussation pattern at the chiasm since most of these identified genes mark half of the retina but not the border between the ventral temporal crescent and the nasal retina.

Differentially expressed genes in the retina that control partial decussation at chiasm

The three currently cloned genes from our group could be candidates involved in the partial decussation pattern in the mouse chiasm.

Based on the searched result, the second sample (TA8.1) has a high sequence homology to the carnitine palmitoyltransferase I in rats. The other two genes TA4.1 and NC2.1 share low homology to other known genes so we suspected that they are novel genes and are specific to the mouse retina. For TA8.1, its seqeunce is similar to carnitine palmitoyltransferase I which is vital for the transport of fatty acid through the mitochrondrial membrane to the matrix of mitochondria for beta-oxidation (Brady et.al., 1992). How the function of carnitine palmitoyltransferase I related to the pathfinding process is not known and all these three genes are

subjected to further analysis in the future. One of the experiments can be done for this purpose is northern blotting. Another approach is in-situ hybridization which has an advantage of more sensitive over the northern blotting.

CHAPTER 5

GENERAL DISCUSSION

This thesis has been dedicated to understand the guidance cues involved in the development of the retinofugal pathway. Three approaches have been applied for this study. In the first approach, we investigated the growth of retinal axons in the chiasm of mouse embryos, both in fixed and living preparation. The major findings include 1) major changes in axon growth were seen in the pre-midline chiasm where uncrossed axons separated from the crossed axons; 2) Retinal axons exhibited constant growth rate in both the pre-midline and post-midline region of the optic chiasm. Based on our studies, axons navigated through the chiasm in pause-and-advance paradigm. Within the pausing periods, active remodeling of growth cone morphology was seen. This active remodeling included branching of growth cones, followed with one of the branches extended while the others retracted. These remodeling processes often led to a change in growth direction. Moreover, this growth behavior was observed in axons at both pre-midline and post-midline chiasm. As retinal axons continuously encounter a complex and changing environment during their growth from retina to their visual targets, we postulate that the change in their growth kinetic and their growth position is a signal implying that axons were actually reading signals from their immediate environment during all these pausing periods.

Besides studying the development of retinofugal pathway, the cues involved in the pathfinding process in the optic chiasm were also studied. Since studies done by various researchers indicated that monocular enucleation reduced the number of uncrossed fibers, axon-axon interaction between the fibers of the retinal ganglion cells from the two eyeballs could be one of the mechanism involved in the pathfinding process (Chan and Guillery, 1993; Guillery et. al., 1995; Taylor and Guillery, 1995). However, the idea is still controversial as there is one reports (Stretavan and Reichardt, 1993) showed that the axon-axon interaction between fibers from the two eyeballs was not required. We thus tried to address the tissue of the immediate effect of monocular enucleation in order to understand whether the axon-axon interaction is really required in the pathfinding process. In our monocular enucleation study, the number of cell bodies of the turning fibers were counted one day after the surgery. Altogether, three age groups were examined and they were the E14, E15 and E16 embryos. Our result indicated that the dependence of axon-axon interaction relied on which age group being studied. Statistical result showed that the early population (E14) of turning fibers were not affected by monocular enucleation (Table 2.1). On the contrary, axon-axon interaction was required for normal development of a correct retinofugal pathway in the late population of uncrossed fibers (E15 and E16). This experiment implies that the early and the late population of turning fibers might rely on different sets of guidance cues for their turning process to occur. The third approach was applying

the differential PCR display to isolate the molecular cues involved in the axonal pathfinding process. Since the axons of crossed and uncrossed fibers were mixed together in the optic chiasm while the cell bodies of the uncrossed fibers were restricted to the temporal crescent region of the retina (Guillery et. al., 1995), active mechanism had to be involved in the pathfinding process. As a result, the retinal ganglion cells must have some instrinsic properties which made the crossed axons response differently from the uncrossed fibers. The differential PCR display was the way we applied to isolate this intrinsic molecular cue in the retinal ganglion cells. By differential PCR display, mRNAs were converted to cDNA so that different expression levels in different parts of retina could be compared . The mRNAs which were differentially expressed in one part of the retina were isolated from the DNA sequencing gel for subsequent analysis. Based on this method, seven DNA fragments were cloned. Three of these DNA fragments were sequenced. One of the DNA fragments was found to have high homology with the gene carnitine Palmitoyltransferase I . The other two DNA fragments were found to be novel genes as there were no high homologous sequences to them in the gene bank.

In order to understand more about the identities of the sequenced gene, we are going to apply in-situ hybridization to analyze our genes. Since the technique in-situ hybridization was tested to be technical possible in our laboratory using pax-6 gene as a template for riboprobe synthesis, our laboratory is currently using this

technique to further analyze the three DNA fragments by examining the expression location of these three genes in the retina. If these genes are really the guidance cues for the pathfinding process, they should be differentially labelled at the temporal crescent region or the nasal retina.

REFERENCE

- Argiro V, Bunge B and Johnson MI (1984) Correlation between growth cone form and movement and their dependence on neuronal age. J Neurosci 4:3051-3062.
- Baker GE and Jeffery G (1989) Distribution of uncrossed axons along the course of the optic nerve and chiasm of rodents. J Comp Neurol 289:455-461.
- Baker GE and Reese BE (1993) Chiasmatic course of temporal retinal axons in the developing ferret. J Comp Neurol 330:95-104.
- Bonhoeffer F and Gierer A (1984) How do retinal axons find their targets on the tectum? Trends Neurosci 7:378-381.
- Bovolenta P and Dodd J (1990) Guidance of commissural growth cones at the floor plate in embryonic rat spinal cord. Development 109: 435-447.
- Bovolenta P and Mason CA (1987) Growth cone morphology varies with position in the developing mouse visual pathway from retina to first targets. J Neurosci 7: 1447-1460.
- Burrill JD and Easter SS Jr (1995) The first retinal axons and their microenvironment in zebrafish: cryptic pioneers and the pretract. J Neurosci. 15 (4): 2935-47.
- Caudy M and Bentley D (1986b) Pioneer growth cone steering along a series of neuronal and non-neuronal cues of different affinities. J Neurosci 6:1781-1795.

- Chan SO and Guillery RW (1993) Developmental changes produced in the retinofugal pathways of rats and ferrets by early monocular enucleations: the effect of age and the differences between normal and albino animals. J Neurosci 13:5277-5293.
- Chan SO and Jen LS (1988) Enlargement of uncrossed retinal projections in the albino rat: additive effects of neonatal eye removal and thalamectomy. Brain Res 461: 163-168.
- Chan SO, Chow KL and Jen LS (1989) Postnatal development of the ipsilaterally projecting retinal ganglion cells in normal rats and rats with neonatal lesions. Developmental Brain Research 49: 265-274.
- Chan, S.O. and Guillery, R.W. (1990). Fibre arrangement in the optic stalk of normal and albino rats. Soc. Neurosci. Abstr. 16:336.
- Chan SO and Guillery RW (1994) Changes in fiber order in the optic nerve and tract of rat embryos. J Comp Neurol 344:20-32.
- Colello RJ and Guillery RW (1990) The early development of retinal ganglion cells with uncrossed axons in the mouse: Retinal position and axonal course. Development 108:515-523.
- Colello RJ and Guillery RW (1992) Observations on the early development of the optic nerve and tract of the mouse. J Comp Neurol 317:357-378.
- Fawcett JW and O'Leary DDM (1985) The role of activity in the formation of topographic maps in the nervous system. Trends Neurosci 8:201-206.

- Godement P, Salaun J and Mason CA (1990) Retinal axon pathfinding in the optic chiasm: Divergence of crossed and uncrossed fibers. Neuron 5:173-186.
- Godement P, Salaun J and Metin C (1987a) Fate of uncrossed retinal projections following early or late prenatal moncular enucleation in the mouse. J Comp Neurol 255:97-109.
- Godement P, Vanselow J, Thanos S and Bonhoeffer F (1987b) A study in developing visual systems with a new method of staining neurones and their processes in fixed tissue. Development 101: 697-713.
- Godement P, Wang LC and Mason CA (1994) Retinal axon divergence in the optic chiasm: Dynamics of growth cone behavior at the midline. J Neurosci 14:7024-7039.
- Guillery RW (1989) Early monocular enucleations in foetal ferrets produce a decrease of uncrossed and an increase of crossed retinofugal components: a possible model for the albino abnormality. J Anat 164: 73-84.
- Guillery RW (1992) Rules that govern the development of the pathways from the eye to the optic tract in mammals. In DM Lam and CS Shatz (eds): Development of the Visual System. MIT Press.

- Guillery RW and Walsh C (1987) Changing glial organization relates to changing fiber order in the developing optic nerve of ferrets. J Comp Neurol 265:203-217.
- Guillery RW, Hickey TL, Kaas JH, Felleman DJ, Debruyn EJ and Sparks DL (1984) Abnormal central visual pathways in the brain of an albino green monkey. J Comp Neurol 226:165-183.
- Guillery RW, Jeffery G and Cattanach BM (1987) Abnormally high variability in the uncrossed retinofugal pathway of mice with albino mosaicism. Development 101: 857-867.
- Guillery RW, Mason CA and Taylor JSH (1995) Developmental determinants at the mammalian optic chiasm. J Neurosci 15:4727-4737.
- Hatini V, Tao W and Lai E (1994) Expression of winged helix genes, BF-1 and BF-2, define adjacent domains within the developing forebrain and retina. J Neurobiology 25: 1293-1309.
- Hill RE, Favor J, Hogan BL, Ton CC, Saunders GF, Hanson IM, Prosser J, Jordan J, Hastie ND and van Heyningen V (1991) Mouse small eye results from mutations in a paired-like homeobox-containing gene. Nature 354: 522-525.
- Holt C (1984) Does timing of axon outgrowth influence initial retinotectal topography in Xenopus. J Neurosci 4: 1130-1152.
- Holt C (1990) A single cell analysis of early retinal ganglion cell differentiation in Xenopus: from soma to axon tip. J Neurosci 9: 3123-3145.

- Holt CE and Harris WA (1983) Order in the initial retinotectal map in Xenopus: a new technique for labelling growing nerve fibers. Nature 301:150-152.
- Honig MG and Hume RI (1985) Interactions between sympathetic preganglionic neurons and sympathetic ganglion neurons in vitro. Soc Neurosci Abstr 11: 98.
- Honig MG and Hume RI (1986) Fluorescent carbocyanine dyes allow living neurons of identified origin to be studied in long-term cultures. J Cell Biol 103:171-187.
- Horton JC and Greenwood MM (1979) Non-retinotopic arrangement of fibres in cat optic nerve. Nature 282:720-722.
- Jacobs JR and Goodman CS (1989) Embryonic development of axons pathways in the Drosophila CNS. II. Behavior of pioneer growth cones. J Neurosci 9:2412-2422.
- Jeffery G (1984) Retinal ganglion cell death and terminal field retraction in the developing rodent visual system. Dev. Brain Res. 13: 81-96.
- Jeffery G and Perry VH (1982) Evidence for ganglion cell death during development of the ipsilateral retinal projection in the rat. Dev Brain Res 2: 176-180.
- Jeffery G, Darling K and Whitmore A (1994) Melanin and the regulation of mammalian photoreceptor topography. Eur J Neurosci 6:657-667.

- Landmesser L and Honig MG (1986) Altered sensory projection in the chick hind limb following the early removal of motoneurons. Dev Biol 218:511-531.
- LaVail JH, Nixon RA and Sidman RL (1978) Genetic control of retinal ganglion cell projections. J Comp Neurol 182: 399-422.
- Liang P and Pardee AB (1992) Differential display of eukaryotic messenger RNA by means of the polymerase chain reaction. Science 257: 967-971.
- Linden R and Serfaty CA (1985) Evidence for differential effects of terminal and dendritic competition upon developmental neuron death in the retina. Neuroscience 15: 853-868.
- Liu ISC, Chen JD, Ploder L, Vidgen D, van der Kooy D, Kalnins VI and McInnes RR (1994) Developmental expression of a novel murine homeobox gene (Chx10): evidence for roles in determination of the neuroretina and inner nuclear layer. Neuron 13: 377-393.
- Marcus RC and Mason CA (1995) The first retinal axon growth in the mouse optic chiasm: axon patterning and the cellular environment. J Neurosci 15:6389-6402.
- Marcus RC, Blazeski R, Godement P and Mason CA (1995) Retinal axon divergence in the optic chiasm: uncrossed axons diverge from crossed axons within a midline glial specialization. J Neurosci. 15: 3716-3729.

- Marcus RC, Wang L-C and Mason CA (1996) Retinal axon divergence in the optic chiasm: midline cells are unaffected by the albino mutation. Development 122:859-868.
- Mason CA and Wang L-C (1997) Growth cone form is behavior-specific and, consequently, position-specific along the retinal axon pathway. J Neurosci 17: 1086-1100.
- Mathers PH, Grinberg A, Mahon KA and Jamrich M (1997) The Rx homeobox gene is essential for vertebrate eye development. Nature 387: 603-607.
- McLoon SC (1991) A monoclonal antibody that distinguishes between temporal and nasal retinal axons. J Neurosci 11: 1470-1477.
- Naito J (1986) Course of retinogeniculate projection fibers in the cat optic nerve. J Comp Neurol 251:376-378.
- Naito J (1989) Retinogeniculate projection fibers in the monkey optic nerve: a demonstration of the fiber pathways by retograde axonal transport of WGA-HRP. J Comp Neurol 284:174-186.
- Nakamura H and O'Leary DDM (1989) Inaccuracies in initial growth and arborization of chick retinotectal axons followed by course corrections and axon remodeling to develop topographic order. J Neurosci 9: 3776-3795.
- O'Leary DDM, Fawcett JW and Cowan WM (1986) Topographic targeting errors in the retinocollicular projection and their elimination by selective ganglion cell death. J Neurosci 6: 3692-3705.

- Pachnis V, Mankoo B and Costantino F (1993) Expression of the c-ret proto-oncogene during mouse embryogenesis. Development 119: 1005-1017.
- Pierre Godement, Josselyne Salaun and Carol A.Mason (1990). Retinal Axon Pathfinding in the Optic Chiasm: Divergence of Crossed and Uncrossed Fibers. Neuron. P 173-186.
- Pierre Godement, Li-Chong Wang, and Carol A. Mason (1994) Retinal axon devergence in the optic chiasm: Dynamics of growth cone behavior at the midline. The Journal of neuroscience. 14(11):7024-7039.
- Quiring R, Walldorf U, Kloter U and Gehring WJ (1994) Homology of the eyeless gene of Drosophila to the small eye gene in mice and aniridia in humans. Science 265: 785-789.
- Rabacchi SA, Neve RL and Drager UC (1990) A positional marker for the dorsal embryonic retina is homologous to the high-affinity laminin receptor. Development 109: 521-531.
- Raper JA, Bastiani MJ, Goodman CS (1983) Guidance of growth cones: selective fasiculation in the grasshopper embryo. Cold Spring Harbor Symp Quant Biol 48:587-598.
- Reese BE and Baker GE (1993) The re-establishment of the representation of the dorso-ventral retinal axis in the chiasmatic region of the ferret. Vis Neurosci 10:957-968.

- Reese BE, Maynard TM and Hocking DR (1994) Glial domains and axonal reordering in the chiasmatic region of the developing ferret. J Comp Neurol 349:303-324.
- Roberts A and Taylor JSH (1983) A study of growth cones of developing embryonic sensory neurites. J Embryol Exp Morphol 75: 31-47.
- Sakaguchi DS and Murphy RK (1985) Map formation in the developing Xenopus retinotectal system: an examination of ganglion cell terminal arborizations. J Neurosci 5:3228-3245.
- Schwartz M and Agranoff BW (1981) Outgrowth and maintenance of neurites from cultured goldfish retinal ganglion cells. Brain Res 206:331-343.
- Sretavan DW (1990) Specific routing of retinal ganglion cell axons at the mammalian optic chiasm during embryonic development. J Neurosci 10: 1995-2007.
- Sretavan DW and Reichardt LF (1993) Time-lapse video analysis of retinal ganglion cell axon pathfinding at the mammalian optic chiasm: growth cone guidance using intrinsic chiasm cues. Neuron 10:761-777.
- Sretavan DW, Feng L, Pure E and Reichardt LF (1994) Embryonic neurons of the developing optic chiasm express L1 and CD 44, cell surface molecules with opposing effects on retinal axon growth. Neuron 12:957-975.

- Sretavan DW, Pure E, Siegel MW and Reichardt LF (1995) Disruption of retinal axon ingrowth by ablation of emrbyonic mouse optic chiasm neurons. Science 269: 98-101.
- Sretavan DW, Reichardt LF (1993) Time-lapse video analysis of retinal ganglion cell axon pathfinding at the mammalian optic chiasm: growth cone guidance using intrinsic chiasm cues. Neuron 10:761-777.
- Stahl B, Muller B, von Boxberg Y (1990) Biochemical characterization of a putative axonal guidance molecule of the chick visual system. Neuron 5:735-743.
- Stone J (1978) The number and distribution of ganglion cells in the cat's retina. J Comp Neurol 180: 753-71.
- Stone J et. al. (1978) Estimate of the number of myelinated axons in the cat's optic nerve. J Comp Neurol 180:799-806.
- Stuermer CAO (1988) Retinotopic organization of the developing retinotectal projection in the zebrafish embryo. J Neurosci 8:4513-4530.
- Tan CC, Hirvonen H, Miwa H, Weil MM, Monaghan P, Jordan T, van Heyningen V, Hastie ND, Meijers-Heijboer H, Drechsler M, Royer-Pokora B, collins F, Swaroop A, Strong LC and Saunders GF (1991) Positional cloning and characterization of a paired box- and homeobox- containing gene from the aniridia region. Cell 67: 1059-1074.

- Taylor JSH and Guillery RW (1994) Early development of the optic chiasm in the gray short-tailed opossum, Monodelphis domestica. J Comp Neurol 350:109-121.
- Taylor JSH and Guillery RW (1995) Effect of a very early monocular enucleation upon the development of the uncrossed retinofugal pathway in ferrets. J Comp Neurol 357:331-340.
- Taylor JSH and Guillery RW (1995a) Does early monocular enucleation in a marsupial affect the surviving uncrossed retinofugal pathway? J Anat 186:335-342.
- Thanos S and Bonhoeffer F (1987) Axonal arborization in the devloping chick retinotectal system. J Comp Neurol 261:155-164.
- Tosney KW, Landmesser LT (1985) Growth cone morphology and trajectory in the lumbosacral region of the chick embryo. J Neurosci 5:2345-2358.
- Trisler GD, Schneider MD and Niarenberg M (1981) A topographic gradient of molecules in retina can be used to identify neuron position. Proc Natl Acad Sci USA 78: 2145-2149.
- Walther C and Gruss P (1991) Pax-6, a murine paired box gene, is expressed in the developing CNS. Development 113: 1435-1449.
- Wang LC, Dani J, Godement P, Marcus RC and Mason CA (1995) Crossed and uncrossed retinal axons respond differently to cells of the optic chiasm midline in vitro. Neuron 15:1349-1364.

- Wilson MA, Taylor JSH and Gaze RM (1988) A developmental and ultrastructural study of the optic chiasma in Xenopus. Development 102:537-553.
- Wizenmann A, Thanos S, Boxberg Y and Bonhoeffer F (1993) Differential reaction of crossing and non-crossing rat retinal axons on cell membrane preparations from the chiasm midline: an in vitro study. Development 117: 725-735.

Figure 1.1A and 1.1B. A confocal micrograph showing a high magnification of E15 labelled axons. An arrow in the photos indicates the midline of the optic chiasm and the scale bar indicates the side of the photos. These diagrams demonstrate a sharp turn made by the turning fibers. The sharp turning ends up with the change of the direction of growth. Also, the turning fibers are characterized by a backwardly pointing branches toward the ipsilateral part of the brain.

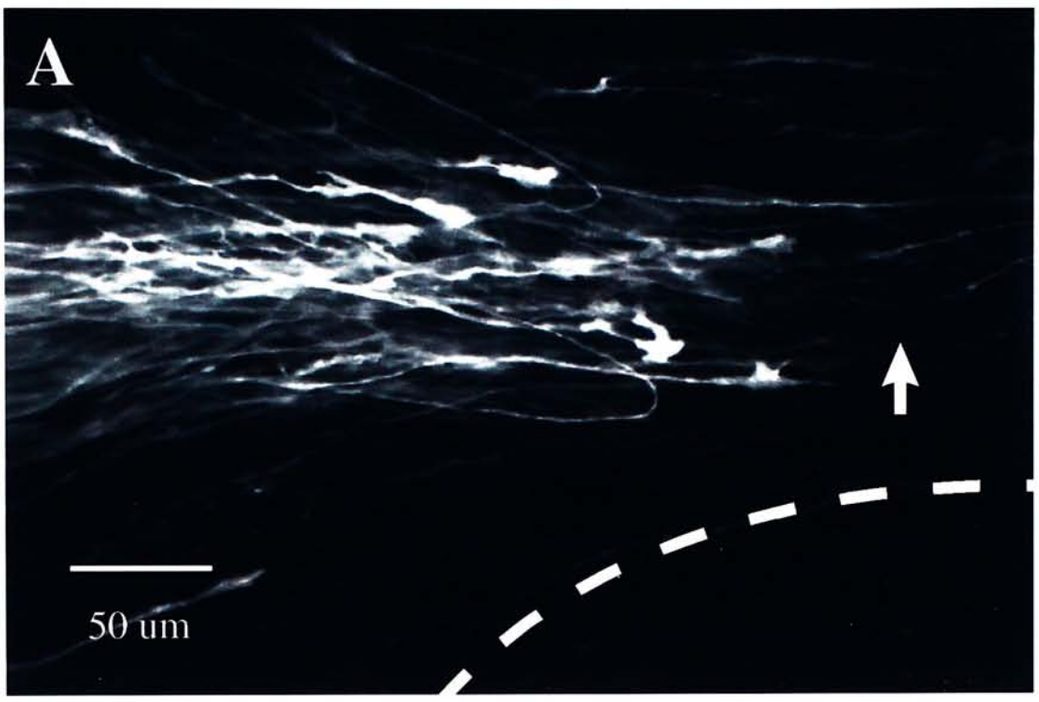
A
50 um

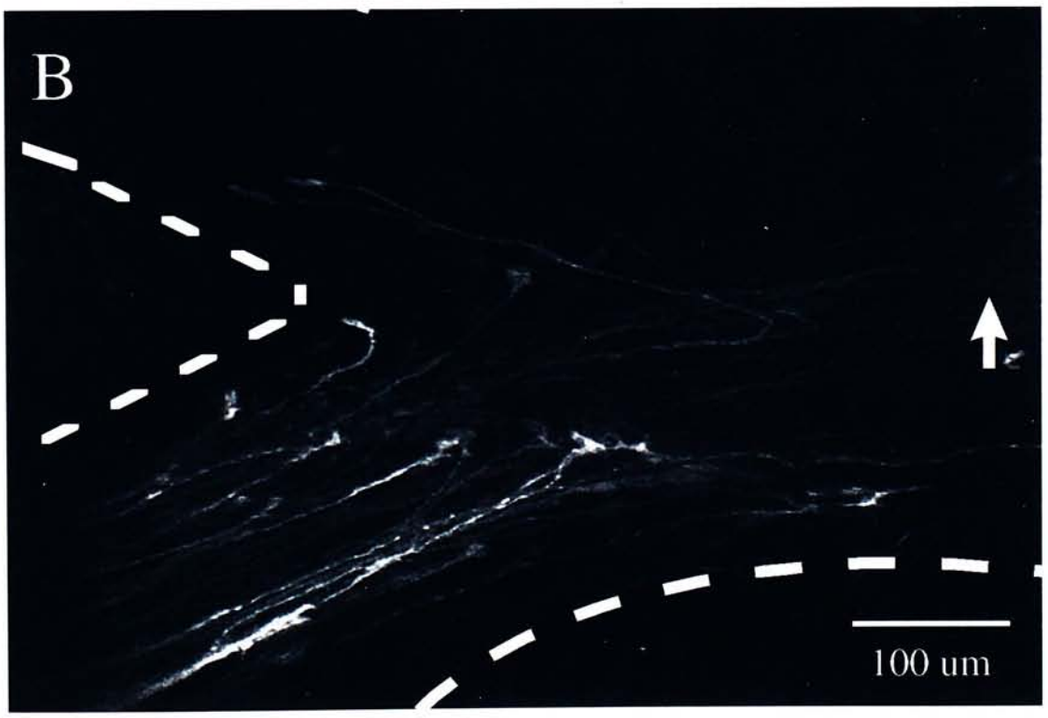
B
100 um

Figure 1.2. Diagrammatic representation of the axon approaching the midline of the chiasm. The inverted arrow at the bottom of the figure indicates the position of the midline of the optic chiasm. The numbers at the right hand side of the figure indicate the period of recording. This axon shows a constant growth at time 0 min to 60 min. During the period from the time of 85 minute to 140 minute, this axon pauses, with the growth cone branches into two parts. One side of the processes was eventaully retracted while the other side of the growth cone continues to extend at 160 min. This morphological change ends up with changing in the direction of growth.

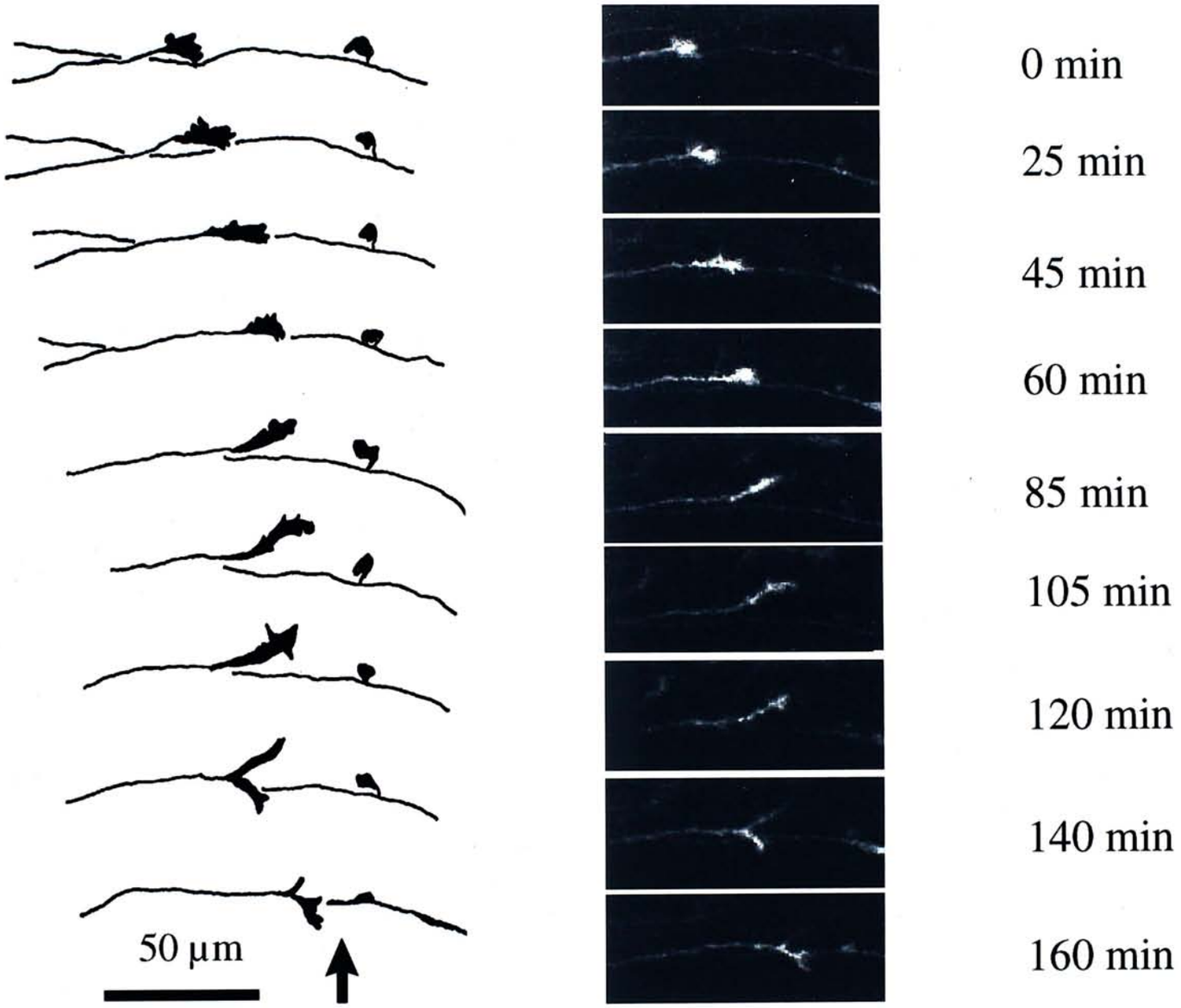
50 µm
0 min
25 min
45 min
60 min
85 min
105 min
120 min
140 min
160 min

Fig 1.3. The axons were imaged at a lower magnification (10x). Most axons displayed a continuous and smooth axon profile. All labelled axons were tipped with a growth cone. One characteristic of axon growth in the premidline chiasm is that each axon had its own tempo of growth. For example, while axon 'A' advanced steadily in the recording period, axons 'C' and 'D' had no obvious increase in length from 0 minute to 80 minute in recording. However, a dramatic increase in length of axon D was observed in the following 20 minutes while axon 'C' was still pausing. Also, all axons underwent a continuous and dynamic change in morphology. For example, axon "B" in Figure 1.3 which turned at the lateral region of chiasm 350μm away from the midline. This axon displayed initially two short appendages from the axon terminal. The appendage pointing towards the midline gradually retracted (at 30 min) and the one that pointed to the ipsilateral tract after a pause for 100 minutes started to grow to the ipsilateral optic tract. Within this pausing period, the growth cone underwent a dynamic modification of its shape which eventually led to its turning.

Premidline

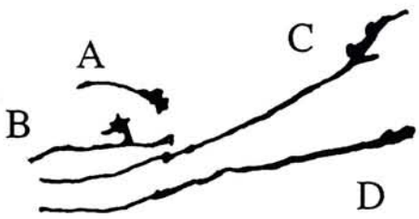

0 min

15 min

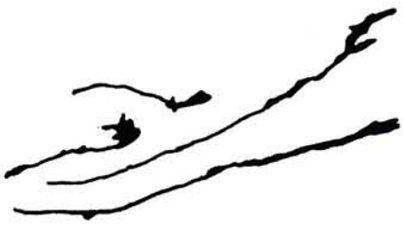

30 min

60 min

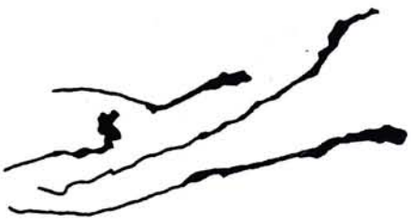

80 min

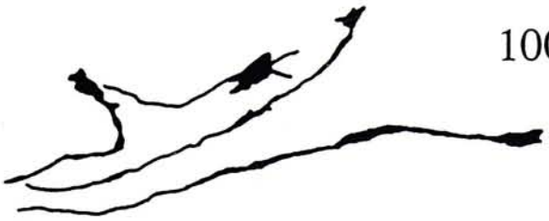

100 min

100µm

Figure 1.4. This figure shows the growth at the midline (indicated by vertical lines) and post-midline regions of the chiasm in E15 embryos. it was noted that axons underwent dynamic changes in growth cone formed in the post-midline chiasm. These growth cones were in general large in size and had a number of processes. The axons were initially growing as 3 fiber fascicles (A-C in Fig. 1.4). Fascicle A was growing at an angle to fascicles B and C which were running in parallel. At the first 80 minutes, these axons continued to grow across post-midine chiasm. There was no obvious change in growth direction and the axons remained as 3 fascicles. However, after 95 minutes in recording, axons in fascicle B started to spread out and grow at different direcitons when they were about 100um away from the midline. An axon from fascicle B deviated caudally at 95 minute in recording and this axon met eventually axon in fascicle A which turned to a rostral direction at 215 minute in recording.

Postmidline

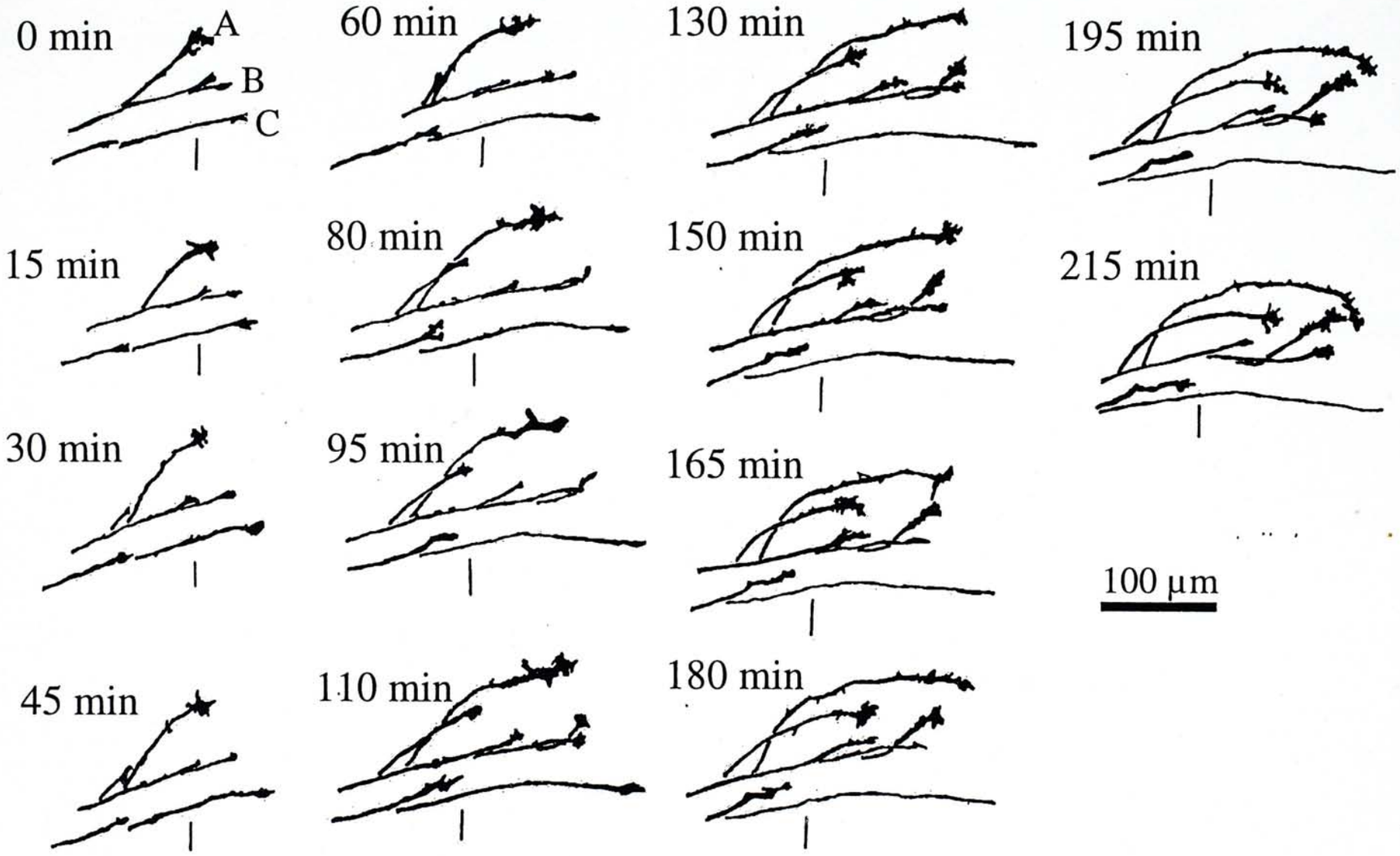

Figure 1.5. This figure contains graphs with the distance of growth against the time of recording. The top 12 graphs are axons located at the pre-midline region while the 11 graphs at the bottom are those axons at the post-midline region. Each graph represents one single recorded axon. The y-axis indicates the distance of growth relative to the starting position. The x-axis indicates the period of recording. The arrow with legend represents the location of the axons with respect to the midline of the optic chiasm. As indicated by the graphs, the growth kinetic for the axons at the post-midline region is very similar to the growth kinetic for those axons in the pre-midline region. All these axons have constant growth rate at different regions of the optic chiasm. Also, interrupts of the growth rates are found in both the pre-midline and post-midline region, as indicated by the small arrow heads. The result shows that reading signals are required in the whole chiasm.

Pre-midline

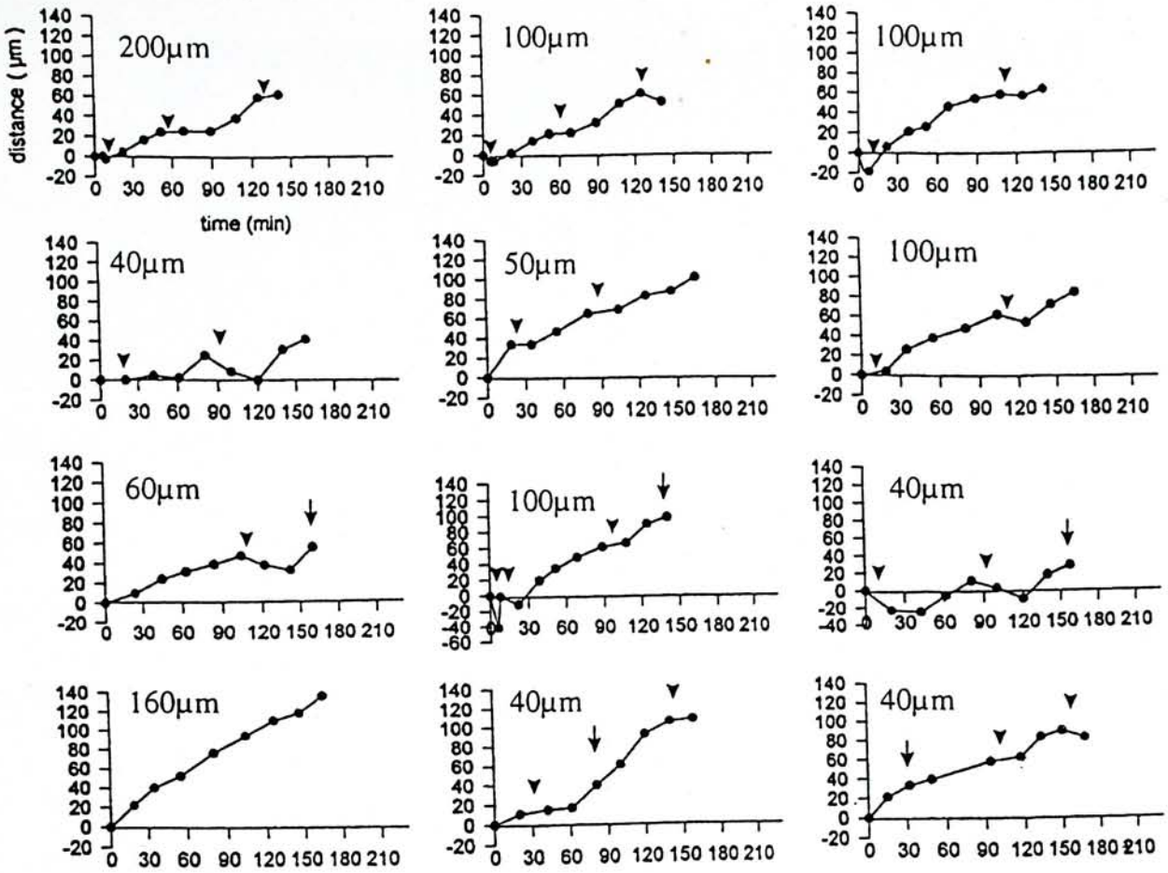

Post-midline

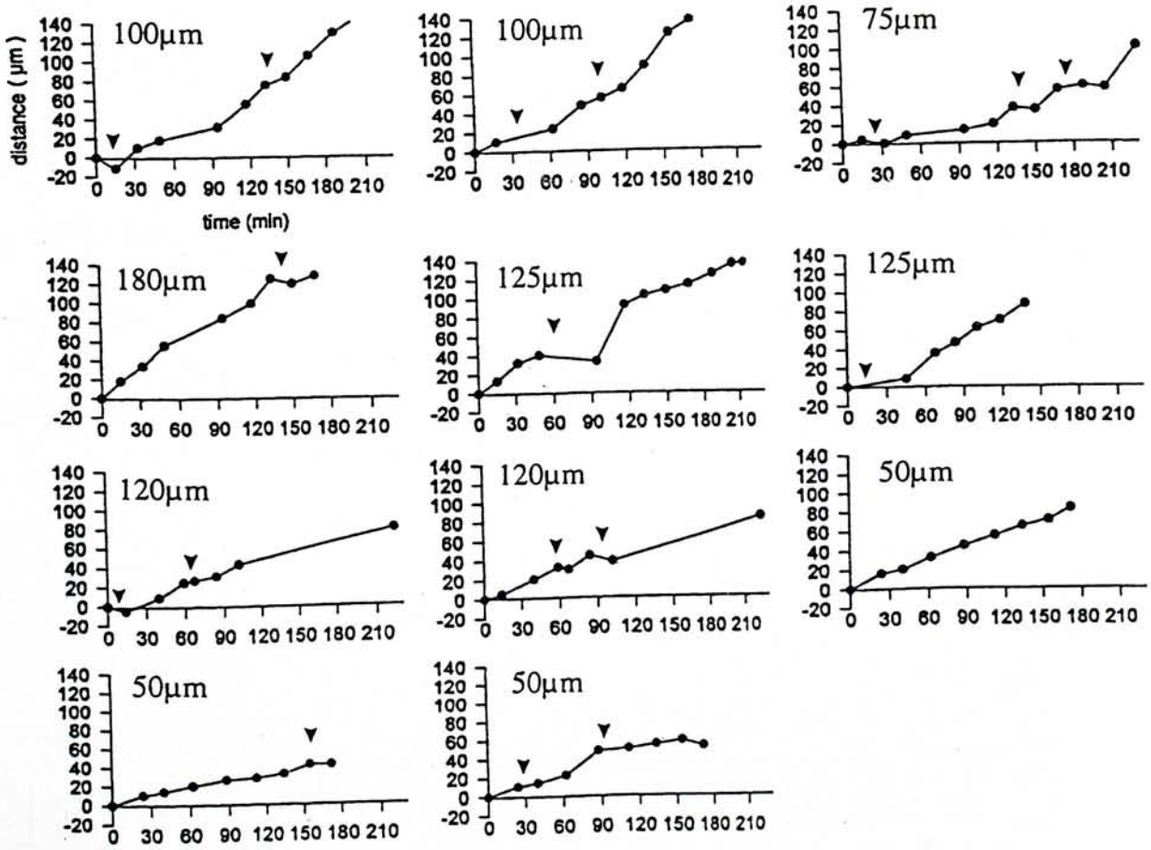

Figure 2.1A. This figure compares two embryos from the same mother. The embryo at the left hand side is a control embryo which does not receive any surgical treatment. The embryo at the right hand side had the left eyeball being removed surgically. Despite the left embryo has two normal eyeballs while the right embryo has only the right eyeball, all other anatomical structures are the same. The result indicates that the surgical method does not has dramatic damage to the embryo which might in turn affect the accuracy of the result interpreted in this experiment.

Fig 2.1B. The right side of a horizontal section of a control embryo is shown. As shown in the photo, the control embryo contains retina (R) which is connected to the optic chiasm through optic stalk (under the label OS). In figure 2.1C, the right side of a horizontal section of a monocular enucleated embryo is shown. Compared with the control embryo, the monocular enculeated embryo has the eyeball being removed. The black spot at the top right hand corner is the pigment epithelium left behind in the original position of the eyeball. The optic nerve which connect the eyeball and the optic chiasm is not found in the photo, suggesting that there should be no outgrowing axons from the eyeball to the optic chiasm


A

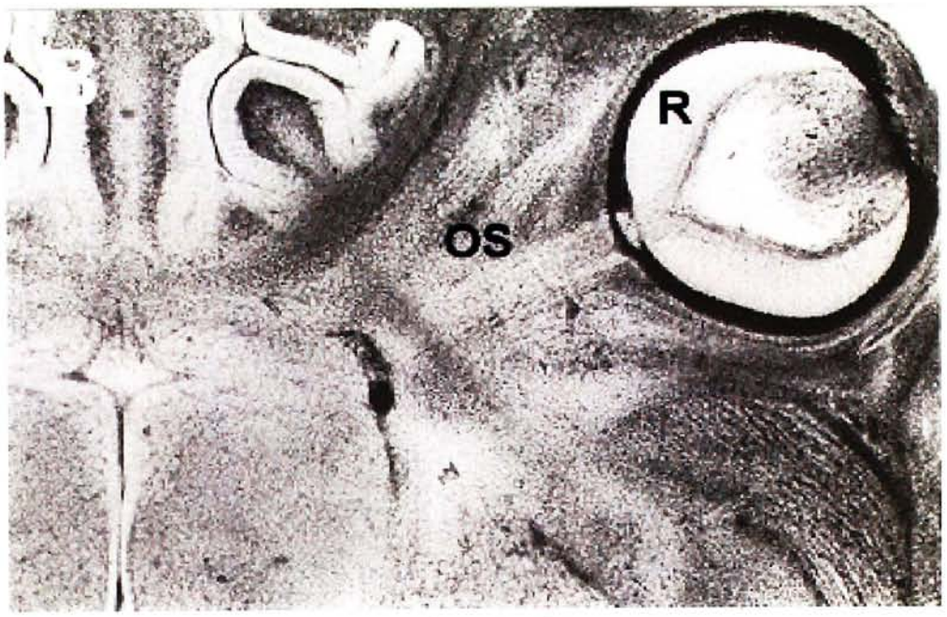
R
OS

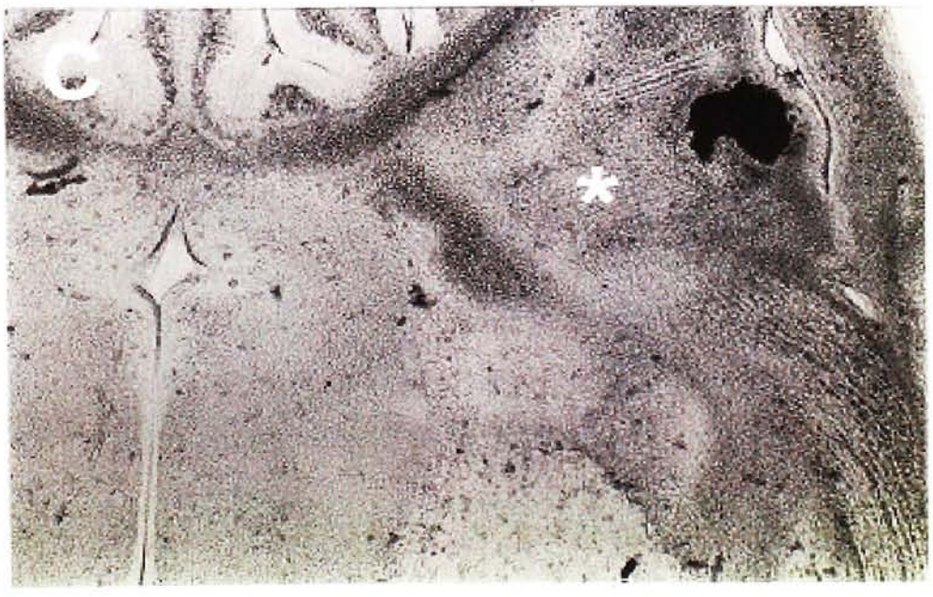
C

Figure 2.2. This figure shows the photos for the crossed fibers in the control group. Figure 2.2A shows a flat-mounted retina at E14. Figure 2.2B shows another flat-mounted retina at E16. As the cell bodies of the crossed fibers distribute all over the retina, the entire retina was labelled. The throughly labelled retina is a good indication that the labelling in the other retina, which was labelled for the cell bodies of uncrossed fibers, is sufficient.


A


B

Figure 2.3. This figure show three photos and their corresponding ages are the embryoic day 14, 15 and 16. The fluorescent dye diI was applied to label the cell bodies of the uncrossed fibers. The result indicates that the early population of uncrossed fibers have their cell bodies spread throughout the retina (figure 2.3a and figure 2.3b). However, for the late population of uncrossed fibers (figure 2.3c), their cell bodies are restricted to the temporal crescent of the retina, which is a region located at the periperal part of the ventral temporal region of the retina, and there are a sudden increases in the number of labeled cells from the opic disk to the perphery of the retina.

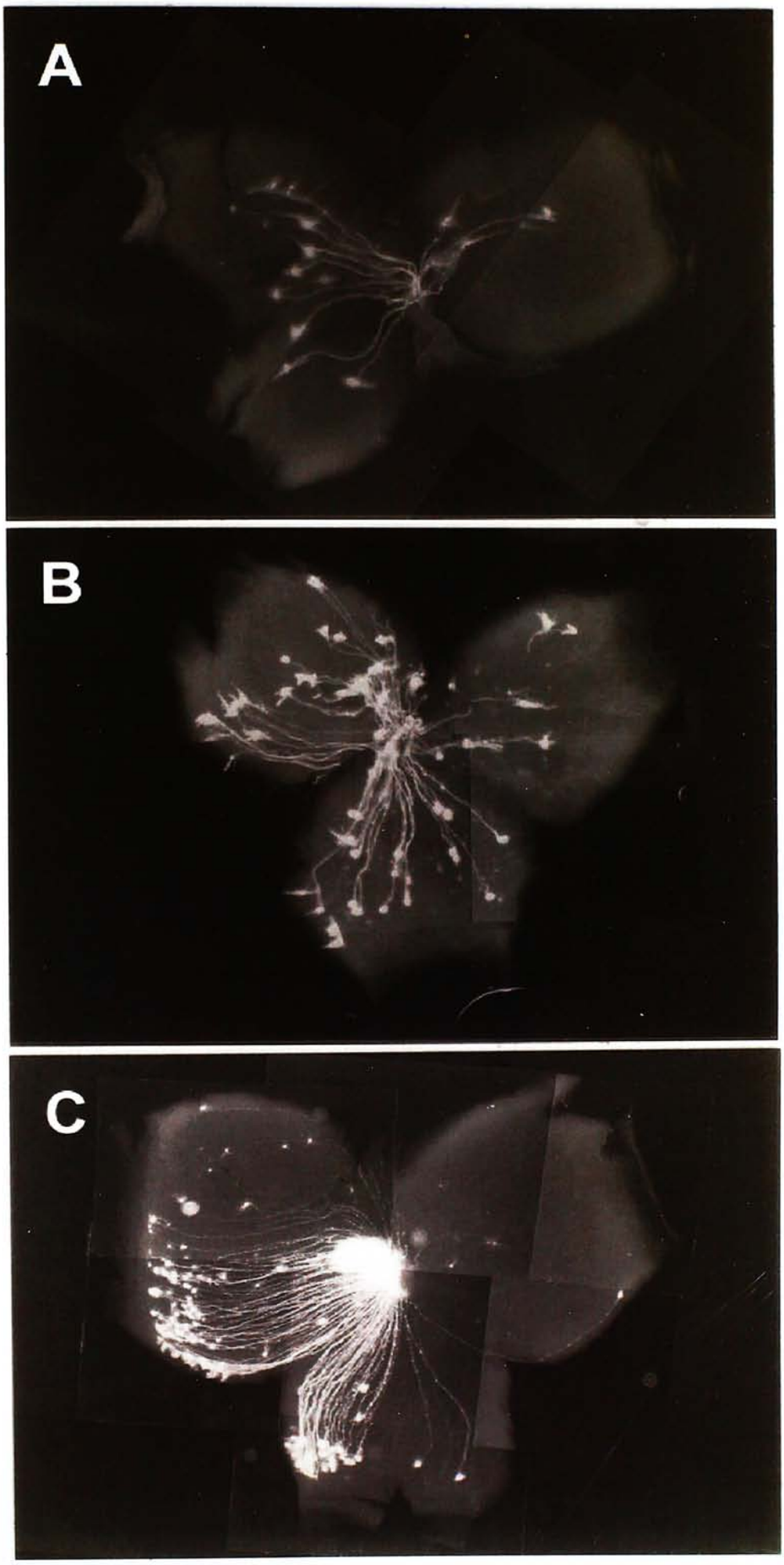
A
B
C

Figure 2.4. This figure is diagrammatic drawings of the retina at E14. The retina aligned at the left hand side is the control group. The retina aligned at the right is the retina received monocular enucleation treatment. The horizontal bar at the left bottom corner is the corresponding scale bar. The black dots inside the retina drawings represent the labelled cell bodies of the uncrossed fibers in the retina. For the orientation of each retina, the doral part of the retina are pointing upward and the temporal part of the retina is pointing toward the right hand side. As shown in the diagrams, the cell bodies spread throughout the retina.

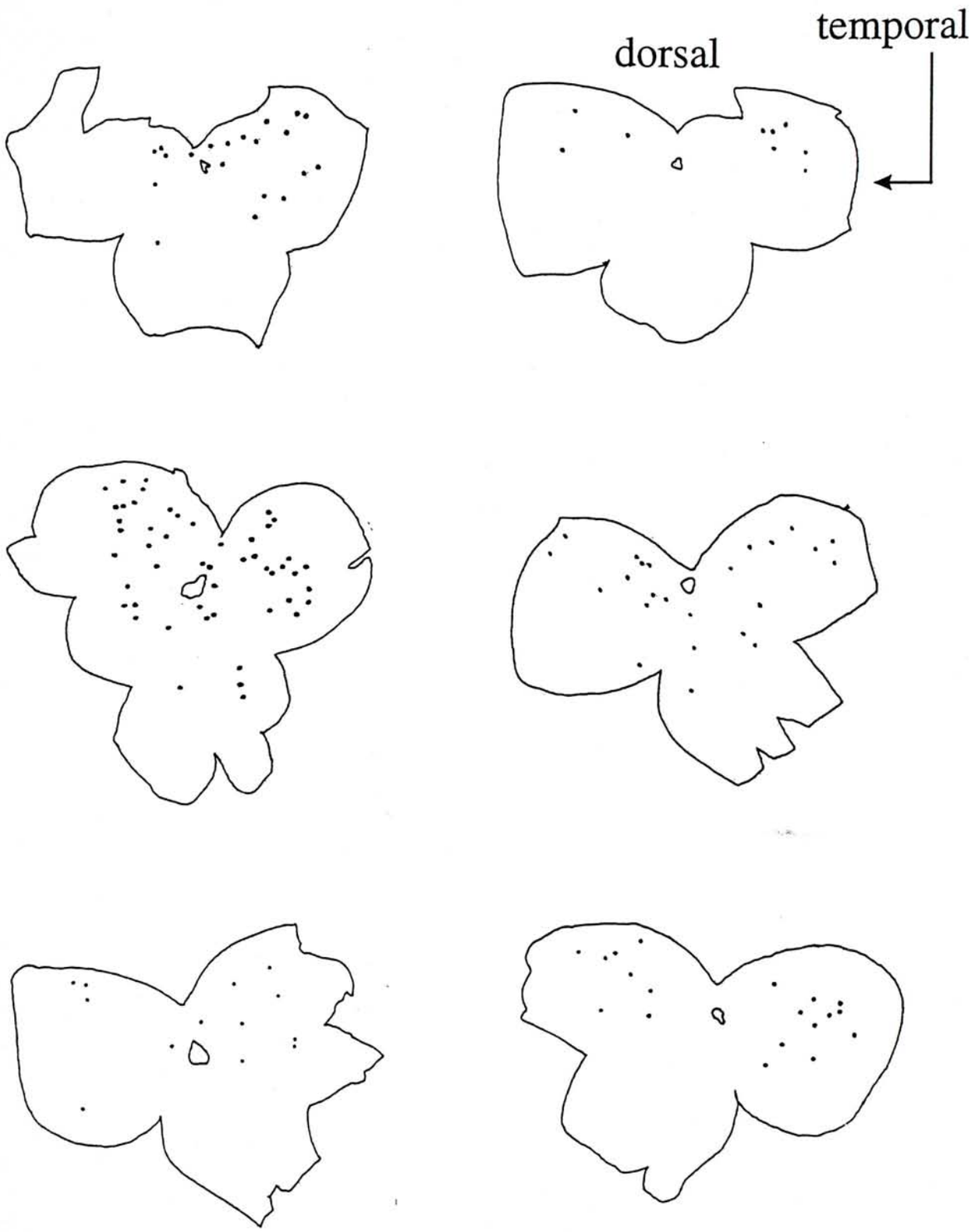
E14, control
E14, monocular
dorsal
temporal
1mm

Figure 2.5. This figure is diagrammatic drawings of the retina at E15. The retina aligned at the left hand side is the control group. The retina aligned at the right is the retina received monocular enucleation treatment. The horizontal bar at the left bottom corner is the corresponding scale bar. The black dots inside the retina drawings represent the labeled cell bodies of the uncrossed fibers in the retina. For the orientation of each retina, the doral part of the retina are pointing upward and the temporal part of the retina is pointing toward the right hand side. As shown in the diagrams, there are increase number of cell bodies in the temporal cresent region (ventral temporal region) of the retina compared with the retina at E14.

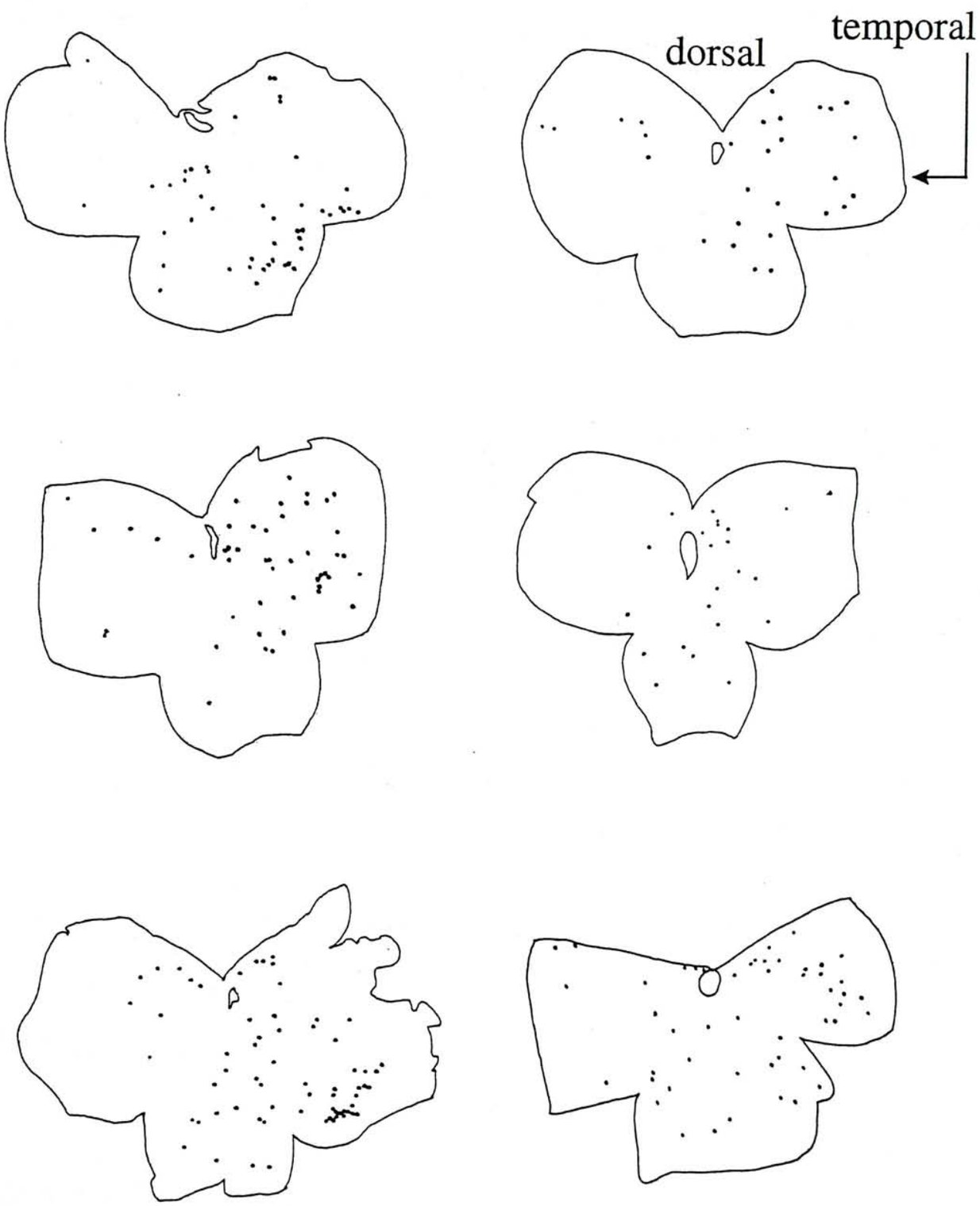
E15, control
E15, monocular
dorsal
temporal
1mm

Figure 2.6. This figure is diagrammatic drawings of the retina at E16. The retina aligned at the left hand side is the control group. The retina aligned at the right is the retina received monocular enucleation treatment. The horizontal bar at the left bottom corner is the corresponding scale bar. The black dots inside the retina drawings represent the labeled cell bodies of the uncrossed fibers in the retina. For the orientation of each retina, the doral part of the retina are pointing upward and the temporal part of the retina is pointing toward the right hand side. As shown in the photos, the cell bodies of the uncrossed fibers are located mainly at the temporal crescent, while just have a few cell bodies located at other part of the retina.

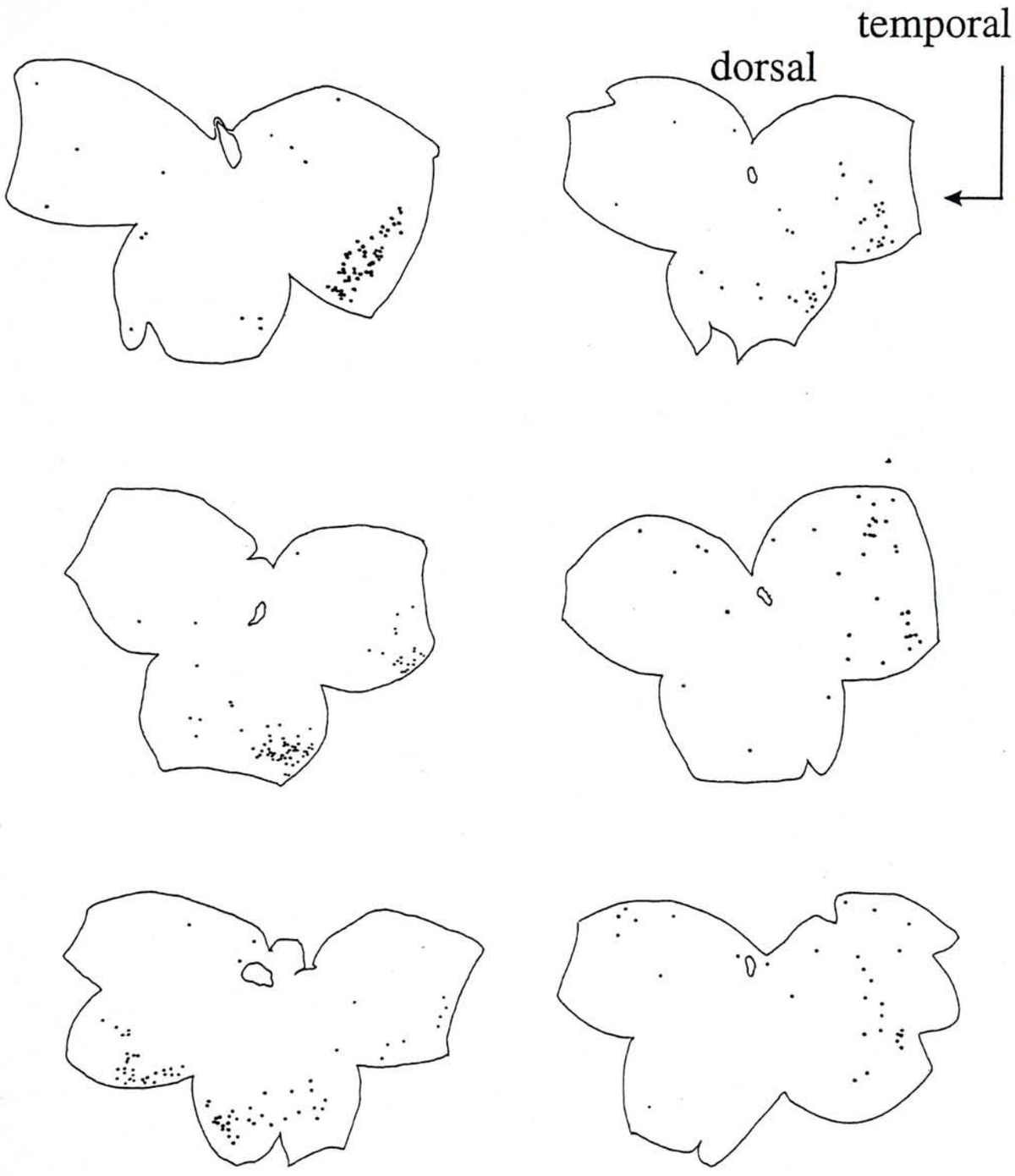
E16, control
E16, monocular
temporal
dorsal
1mm

Fig 3.1 This figure shows the diagrammatic representation of the distribution of ipsilaterally projecting retinal ganglion cells. At E15 to E16 retina, the cells of the uncrossed fibers located mainly at the peripheral region of the ventral temporal part of the retina. For the cell bodies of the crossing fibers, their cell bodies covering the rest of the retina.

Distribution of ipsilaterally projecting retinal ganglion cells

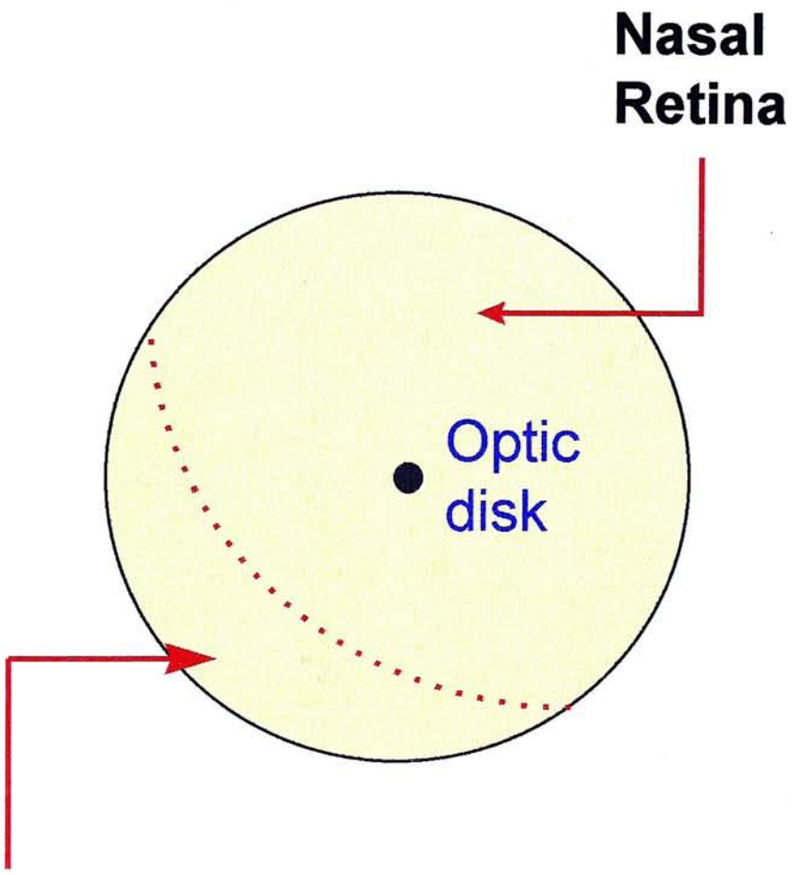

Ventral temporal retina :

a region where the majority of turning axons arise

Fig 3.2. This figure shows the DNA sequencing gel of the differential PCR display. Each pair of lanes shown in the gel are the cDNA patterns in the nasal retina (N) and the ventral temporal retina (T), as indicated by the labels at the top of the gel image. In general, the expression patterns in both nasal and temporal region of the retina are the same. However, there are some bands only found in one region of the retina but not the other. These band are isolated from the DNA sequence gel for subsequent analysis.

Differential display

N : Nasal retina

V : Ventral temporsal retrina

Figure 3.3. This figure shows the agarose gel analysis of DNA fragments after PCR amplification. The bands are the re-amplified DNA from the gel of Differential PCR display. The labels at the top of the gel image are the names given to the samples. The numbers at the left hand side of the gel image are the molecular weights of the DNA marker. The molecular size of each amplified band was estimated by comparing with the corresponding bands of the DNA marker. The analysis of the size of each band was done and summarized in Table 3.1.

Extracted cDNA

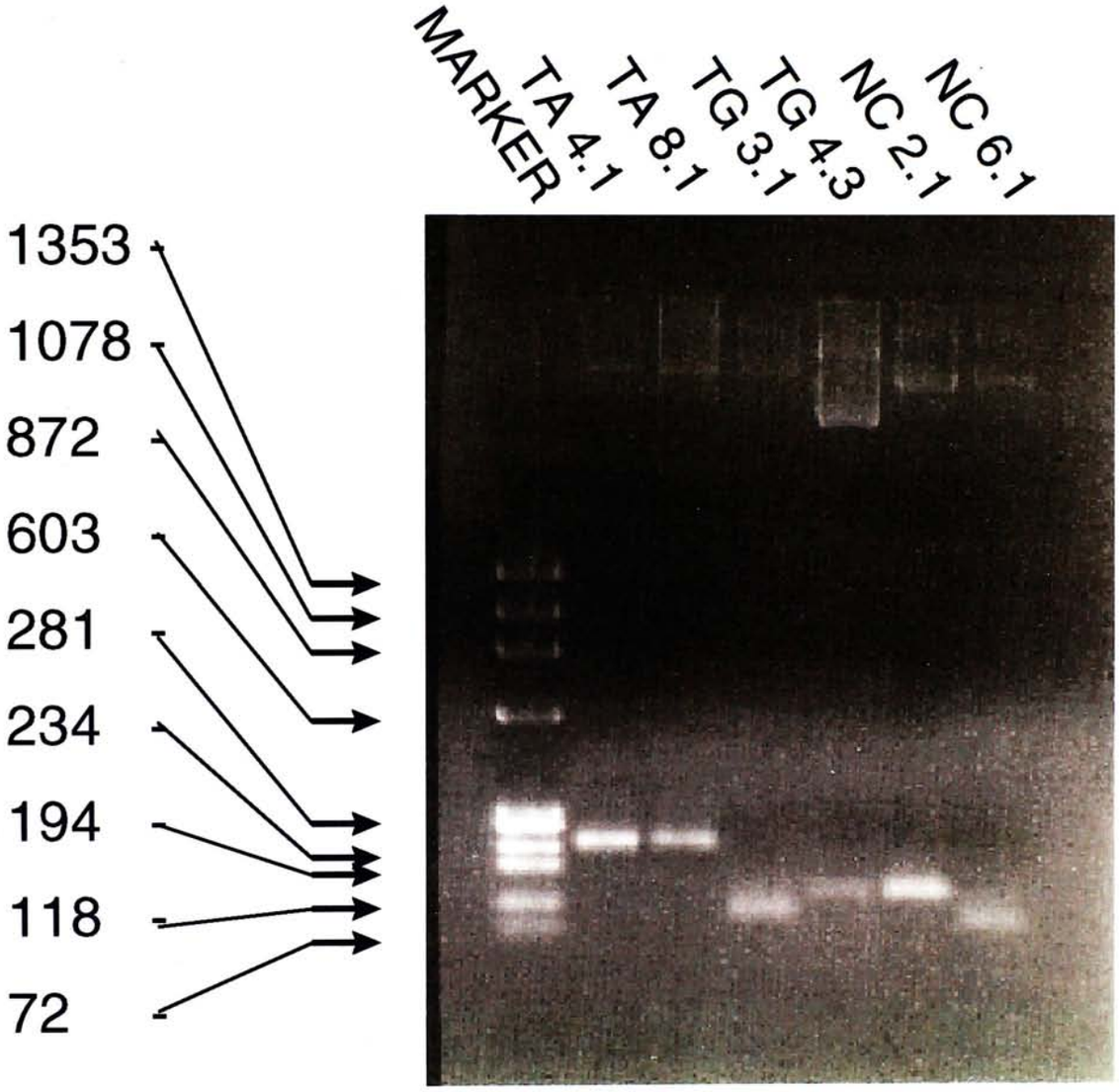

Figure 3.4. This figure shows you the DNA sequence of the sample one (TA4.1), sample 2 (TA8.1) and sample 3(NC2.1). The double underlined sequences are a Hind III restriction sites. The single underlined region is the vector's sequence. The sequence flanked by the restriction sites is the insert. For the bases of the DNA, they are represented by:

A : adenine

T : thymine

G : guanine

C : cytosine

N : unknown base

The diagrammatic representation of the samples one is shown at the top of figure 3.4.

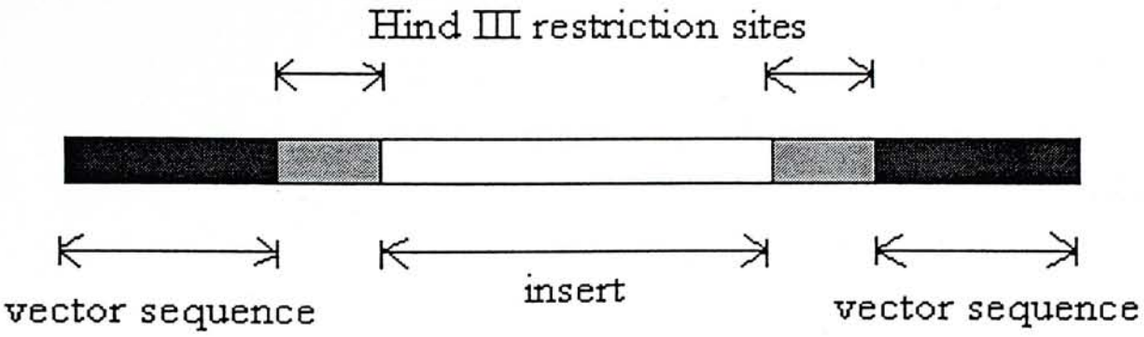

Sample 1: sequence of TA4.1 (154 bp)

TGATAGGAGTCATAGGCCATGAAGGATTCAGGNAGCTTTTNAACGGTAATGGCTAT
GTTTTTAAATGGATTTATACATTTTAATATTTTAAGTNNCCNTGATATTTCTGTTT
GGTTTTTCACAAAATTACGATTGTTGAGTTCCTATTATTAAACAGCTTTTTGCTAC
ACTAAAAAAAAAAAGCTTCCTTTNAGGTANTTNAGACCGCCATCTATGACC

Sample 2: sequence of TA8.1 (158 bp)

ATTCAANAAANTGGTNCATANATGGCGGTCANNANTACCTGAAANGAAGCTTTTAC
CGCANCCNAGNNNCGAATTTGGTTTTCTAATCTGTCCATTGCATGTAAATACCATA
TGCTGTTTGGATATAAATCTTANAAATGCATGTGTGAACNAATATAGCTGANCCAT
TAATAAAACATTAATCCCGCCTAAAAAAAAAAGCTTCCTGAATCCTTCATGGCCTA
TGACTCCTATCAACGGGAACTGCAAAATTATCGGTGTGTCGGAA

Sample 3: sequence of NC2.1 (86 bp)

GGTCATAGNTGGCGGTCAGAAGTACCNGAAAGGNAGCTTTNGACTGTGTAANATGT
GGNAAAGACTCNGCNTGTTGGTCNAACCATAAACTGTCCTAATTTTCGNAAAAAAA
AAAGCTTCCTGAATCCTTCATGGCCTATGGCACCTAACAACCGGAACTGCAA

Table 1.1. This table summarized the result of growth rate for the axons located at the pre-midline and post-midline region. The result indicates that the growth rate of axons has a range, from about 0.23 to 0.83 um/min. the mean of the growth rate is about 0.51 um/min. The corresponding graphs for all these axons are shown in figure 1.5.

Table 1.1. Growth kinetics of retinal axons at the chiasm

Position	Number of Axons	Growth Rates (μm/min)		
		Minimum	Maximum	Mean ± S.E.
Pre-midline	14	0.24	0.84	0.50 ± 0.05
Post-midline	12	0.22	0.81	0.52 ± 0.06

Table 2.1. This table is a. summary of the number of cell bodies of the uncrossed fibers done by our group. The cell bodies are grouped into different age groups: E14, 15 and E16. For each age groups, two different groups of embryos are studied and they are the control group and the monocular enucleated group. During analysis, cell bodies counted from the retina are further classified into the temporal crescent region (TC) and also the nasal retina (NR). Based on statistical analysis using Mann-Whitney nonparametric test, those numbers have significant difference between the control and treated groups are marked with "*".

Table 2.1 Immediate effect of early monocular enucleation on the uncrossed retinofugal pathway

Animal	Cases	Number of ipsilaterally projecting cells (mean±SEM)		
		TC	NR	Total
E14				
Control	8	0	33.50±8.05	33.50±8.05
Enucleate	3	0	18.67±4.84	18.67±4.84
E15				
Control	7	37.43±18.33	50.00±8.37	87.43±23.06
Enucleate	6	0	30.00±6.97	30.00±6.97*
E16				
Control	9	96.89±10.09	52.00±13.62	148.89±20.15
Enucleate	6	29.00±10.80*	24.33±5.54	53.33±10.18*

TC: Temporal crescent
NR: Nasal retina
SEM: Standard error of means

* With statistically significant difference, $p<0.05$, using Mann-Whitney nonparametric tests

Table 3.1. This table summarizes the size of the re-amplified samples for inserts isolated from the DNA sequence gel. The size of the inserts were comparing with the expected sizes estimated from the DNA sequencing gel. Only those inserts which have size matched are used for subsequent analysis. These approaches can eliminate the fake DNA inserts which are not from the Differential PCR display. Based on the result, the sample one, two and five had matched size and were used for further analysis.

Table 3.1

Sample	Expected size of sample after PCR	Actual size after PCR	Match
1) TA4.1	236	275	+
2) TA 8.1	238	275	+
3) TG3.1	276	130	x
4) TG4.3	320	-	-
5) NC2.1	200	194	++
6) NC6.1	300	140-150	x

- "+" means the level of matching.
- "-" means the DNA which cannot be amplified by PCR method.
- "x" means not matching.